

The Dynamics of Interstellar Asteroids and Comets within the Galaxy: an Assessment of Local Candidate Source Regions for 1I/‘Oumuamua and 2I/Borisov

TIM HALLATT^{1,2,3} AND PAUL WIEGERT^{1,4}

¹*Department of Physics and Astronomy, The University of Western Ontario, London, Ontario, ON N6G 2V4, Canada*

²*Department of Physics, McGill University, Montréal, Québec, QC H3A 2T8, Canada*

³*McGill Space Institute; Institute for Research on Exoplanets (iREx); Montréal, Québec, Canada*

⁴*The Institute for Earth and Space Exploration (IESX), London, Ontario, Canada*

(Received November 7, 2019; Revised; Accepted)

Submitted to AAS journals

ABSTRACT

The velocity of interstellar asteroid ‘Oumuamua with respect to the Local Standard of Rest of our Galaxy is low, which implies it is young, at least if it was ejected during its host star’s protoplanetary phase. With this young age as our hypothesis, we assess possible origin systems for the interstellar asteroid in two ways.

First, by modelling ‘Oumuamua’s past trajectory under the influence of the galactic tide and the disk heating (ie. scattering) to assess how far back one can reliably expect to trace its orbit. The stochastic nature of disk heating means that a back integration of ‘Oumuamua can only expect to be accurate to within 15 pc and 2 km/s at -10 Myr, 100 pc and 5 km/s at -50 Myr, and 400 pc and 10 km/s at -100 Myr, sharply limiting our ability to determine a precise origin. However, we can show that if ‘Oumuamua was ejected at low (~ 1 km/s) speed, as is likely for most ejection processes, ‘Oumuamua’s origin system is currently within 1 kpc of Earth. This would place the origin system nearby within the local Orion Arm, and thus relatively easily accessible to telescopic study. This provides strong motivation for continued efforts to determine ‘Oumuamua’s place of origin, because that system could be studied in detail and shed light on the nature of this unusual asteroid.

Second, with this initial assessment in hand, we perform a backwards integration of ‘Oumuamua’s trajectory accounting for uncertainty in its and the candidate source regions’ speed and position where possible, to assess potential candidate regions. The Gaia DR2 catalog and the SIMBAD catalog were considered, with particular emphasis on young systems as detailed in the Catalog of Suspected Nearby Young Stars (Riedel et al. 2018) and moving groups as compiled in Gagné et al. (2018). Though disk heating prevents making any but a statistical link to local star-forming regions and moving groups, our best candidates are the Carina and Columba moving groups, the Lupus SFR, the T-Tau stars V391 Ori and BD+11 414, and the M dwarf GJ 1167 A. ‘Oumuamua passed through at least a considerable subset of the Carina and Columba moving groups at a time comparable to their ages, making it perhaps the most plausible source region, if the asteroid was ejected by the planet-forming process.

During the writing of this paper, a second interstellar comet 2I/Borisov was discovered. Though unlikely to be young due to its high velocity with respect to the LSR, we performed a similar analysis and found three stars in the Ursa Major group (GJ 4384, EV Lac, and GJ 102), one brown dwarf of the AB Dor group (2MASS J03552337+113343), and 8 Gaia DR2 stars (including EV Lac) to have plausible encounters at speeds <30 kms⁻¹ and within 2 pc. We do not find any plausible encounters at speeds lower than 13 kms⁻¹.

Keywords: interstellar comets - 1I/‘Oumuamua - 2I/Borisov - Milky Way

1. INTRODUCTION

The first detection of an interstellar object (ISO) occurred on October 19, 2017 (Meech et al. 2017). The Panoramic Survey Telescope And Rapid Response System (Pan-STARRS1) performed the initial detection. Dubbed ‘*Oumuamua*, loosely meaning *Messenger From Afar*, its discovery has ushered in a new era in the study of planetary objects and planet formation.

The population of known interstellar objects such as ‘*Oumuamua* has been predicted to grow significantly over the next few years with the advent of the Large Synoptic Survey Telescope (Moro-Martín et al. 2009). ISOs therefore represent a new class of object, and may provide unprecedented insight into the dynamics and materials of the systems which produce them. By studying their compositions and dynamics as they pass through the solar system (or impact Earth in the case of interstellar meteors), knowledge of the ISOs’ present conditions can be tied to knowledge of their original birthplaces, provided they can be traced backwards in time to their home systems.

Understanding the origins of interstellar asteroids and comets requires an examination of their dynamics within the context of our Milky Way galaxy. Our broader purposes here are 1) to bring the established principles of galactic stellar dynamics to bear on the question of the origin of these much smaller yet related bodies; and 2) tabulate a catalog of plausible galactic source regions with well-established positions and velocities, to serve as the basis for comparison for this and future studies of interstellar bodies. Here the Gaia DR 2 catalog (Gaia Collaboration et al. 2018, 2016), SIMBAD (Wenger et al. 2000), as well as the Catalog of Suspected Nearby Young Stars (Riedel et al. 2018) and members of nearby moving groups compiled in Gagné et al. (2018) that contain full position and velocity information were used.

This paper has three specific purposes. First, to quantitatively assess how far back in time we can trace the path of ‘*Oumuamua* within the context of galactic dynamics. For this purpose we will model the Milky Way’s gravitational potential, and the gravitational scattering processes which cause ‘disk heating’ —the gradual increase in the velocity dispersion of disk stars over the course of time— to assess their influence on the path of ‘*Oumuamua*. The phenomenon of disk heating is well documented and the age-velocity dispersion relation (AVR) has been well-established through the study of local stars. We determine that the path of our ISO can be traced back with some reliability perhaps as far back as 50 Myr or more. Secondly, the low velocity of ‘*Oumuamua* with respect to the Local Standard of Rest (3-10 km/s, Schönrich et al. (2010); Coşkunoğlu et al. (2011)) hints that it might in fact be young. Adopting this as our working hypothesis, we model ‘*Oumuamua*’s path through the Milky Way to assess how close its origin point might be. If ‘*Oumuamua* is indeed as young as its low peculiar velocity indicates, we find that its origin is likely to be currently within 1 kpc of the Earth, and thus available for detailed study if we can identify it. Thirdly, we attempt to identify the source region of ‘*Oumuamua* (still under the assumption that it is young) by modelling the path of ‘*Oumuamua* and known astrophysically-likely regions in near-Sun space (YSOs, molecular clouds, etc) to look for close approaches while accounting for the disk heating process. We do find particularly promising candidate source regions in the Carina and Columba moving groups, as well as the Lupus star-forming region (SFR). The discovery of comet 2I/Borisov¹ during this work lead us to consider its motion within the Galaxy as well. However, its higher speed with respect to Local Standard of Rest indicates an older age, making tracing it back to its origin even more difficult. Nonetheless we performed a similar analysis on its past trajectory and report on some close encounters, though none are at low enough velocity to allow a compelling linkage.

1.1. Possible sources of ISOs

A number of possible sources of ISOs have been proposed in previous work, with recent developments inspired by the discovery of ‘*Oumuamua*. Such investigations of ejection of material from planetary systems have taken place within a number of contexts. Planetesimals interacting with young planets (Fernández & Ip 1984), the dynamics and formation of Oort Clouds and the comets and asteroids which constitute them (Duncan et al. 1987; Brassier & Morbidelli 2013), asteroidal and cometary ejecta from both binary star systems (Jackson et al. 2018), and white dwarf tidal disruption events (Rafikov 2018), and even ejection of smaller-scale dust from young main sequence stars, asymptotic giant branch (AGB) stars, and young stellar objects (YSOs) (Murray et al. 2004) have been studied in some detail.

¹ Minor Planet Electronic Circular 2019-S72 <https://minorplanetcenter.net/mpec/K19/K19S72.html>

Here we will not concern ourselves with the exact mechanism of ejection, except to note that, whatever the process, more energetic events are typically rarer than lesser ones. Thus ejection events just above the system’s escape velocity are expected to be more common, and thus lower excess velocities are more likely. Thus a past encounter between ‘Oumuamua and a particular astrophysical system at a low relative velocity will be considered more consistent with an origin there than an encounter at higher relative velocity, all else being equal.

1.2. *Disk heating and ‘Oumuamua’s speed with respect to the Local Standard of Rest*

Stars form mainly in giant molecular clouds, which are confined more or less to the galactic plane with a scale height of about 80 pc and a velocity dispersion ≈ 5 km/s (Jog & Ostriker 1988; Gammie et al. 1991; Ferrière 2001). The distribution of stars in the Milky way’s disk is much broader (300 pc and 25-35 km/s for the old thin disk near the Sun (Bland-Hawthorn & Gerhard 2016)). This is attributed to “disk heating”, the scattering of stars by molecular clouds or spiral arms as they travel together through the galactic potential. This process has been well studied both theoretically and observationally, though the relative contributions of giant molecular clouds (GMC) and spiral structure remains unclear (encounters with individual stars provide negligible scattering, (Binney & Tremaine 1987)). Disk heating can be modelled rather well as a random walk with some initial velocity dispersion (Wielen 1977). In particular, the phenomenon has a clear trend with age; young stars have much lower deviations from the LSR than older populations (Holmberg et al. (2009), Figure 7).

‘Oumuamua would be subject to the same scattering processes as stars, and so the stellar age-velocity relation can be used to estimate its age. Feng & Jones (2018) present an analysis of ‘Oumuamua’s velocity relative to the Local Standard of Rest (LSR). They note it deviates just 3 km s⁻¹ from the LSR defined by Schönrich et al. (2010), and less than 10 km s⁻¹ from that defined by Coşkunoglu et al. (2011). We find a value of 11.5 kms⁻¹ for our adopted LSR. These values are lower than are usually covered by galactic age-velocity relations, but imply an age less than 1 Gyr e.g. an extrapolation of (Holmberg et al. 2009) Figure 7 yields an age ~ 100 Myr; (Robin et al. 2017) reports an age less than 150 Myr for the subcomponent corresponding to ‘Oumuamua’s velocity. Other authors have also argued ‘Oumuamua’s small deviation from the LSR indicates it has undergone only a small amount of dynamical perturbation throughout its journey (Gaidos et al. 2017).

‘Oumuamua’s low velocity with respect to the LSR is a clue that it may be young, though not proof: it could indeed be as old as the Milky Way itself, but the probability of drawing a value less than or equal to 11.5 km/s from a Maxwell-Boltzmann distribution with a most probable value of 30 km/s is only 0.04. In the absence of any other information we will adopt and examine here the hypothesis that ‘Oumuamua is young (less than 100 Myr old).

We note the useful fact that 1 km s⁻¹ ≈ 1 pc Myr⁻¹. This allows us to quickly estimate that if ‘Oumuamua was ejected at low speed (say 1 kms⁻¹) from its birth system 100 Myr ago, ‘Oumuamua has travelled only about 100 pc since it was ejected, or in other words, the source of ‘Oumuamua is 100 pc away from the Earth currently (since ‘Oumuamua is nearby). Of course, during that 100 Myr both ‘Oumuamua and its home system will have completed 40% of an orbit around the Galaxy, travelling about 20,000 pc as they do so, but their displacement relative to each other is much less. Though this simple analysis has not yet accounted for the random walk of disk heating, the two reasonable assumptions that 1) ‘Oumuamua’s low velocity with respect to the LSR implies it may be young and 2) that low ($\lesssim 1$ kms⁻¹) ejection speed processes are more efficient than high-speed ones, lead us to examine a possible origin for ‘Oumuamua in the local galactic neighbourhood.

2. MODEL

2.1. *Our model of the Milky Way Galaxy*

We treat the gravitational field of the galaxy using a time-independent, three-component function as developed by Miyamoto & Nagai (1975). Accounting for contributions from the galactic disk, bulge, and halo produces, in galactocentric cylindrical coordinates,

$$\Phi_{gal} = \Phi_d + \Phi_b + \Phi_h, \quad (1)$$

$$\Phi_{gal} = - \sum_{i=d,b,h} \frac{GM_i}{\sqrt{R^2 + (a_i + \sqrt{z^2 + b_i^2})^2}}, \quad (2)$$

as widely used in previous studies (for example Bailer-Jones et al. (2018) and Zuluaga et al. (2018)). The length scales a and b are tuned to reflect the geometries of the galactic disk, bulge, and halo components. Setting $b \ll a$

we recover a Kuzmin potential which we use to model the flat geometry of the disk, while setting $a \ll b$ produces a Plummer sphere which models the spherical bulge and halo components. We take the values for a , b and the mass components for each geometry from [Dauphole & Colin \(1995\)](#). Although newer mass estimates have been made ([Portail et al. \(2015\)](#) estimate a portion of the bulge mass, and [Bland-Hawthorn & Gerhard \(2016\)](#) record estimates for the dark matter and disk masses, as well as characteristic lengths for the various geometries), we estimate that those of [Dauphole & Colin \(1995\)](#) are generally within a factor of two of these newer values. Changing them does not significantly affect the results of integrations through this potential. The constants used are summarized in Table 1.

All coordinate transformations are done using `AstroPy`, version 3.1.2. Astrometry for all stars and ‘Oumuamua is instantiated in the ICRS frame, and transformed to a galactocentric cylindrical frame via the `transform_to` and `represent_as` methods before numerical integration. In defining its Galactocentric frame, `AstroPy` derives the galactic center position from [Reid & Brunthaler \(2004\)](#), the solar distance from galactic center from [Gillessen et al. \(2009\)](#) (which has been updated from 8.2 kPc to 8.3 kPc in [Bland-Hawthorn & Gerhard \(2016\)](#)), the sun’s height above the galactic plane from [Chen et al. \(2001\)](#), the solar peculiar velocity from [Schönrich et al. \(2010\)](#) (though [Bland-Hawthorn & Gerhard \(2016\)](#) give a slightly different estimate based on averaging results from multiple studies), and the circular velocity at the solar radius from [Bovy \(2015\)](#). These constants are also included in Table 1.

Table 1. Parameters Defining Galactic Geometry and `AstroPy`’s Galactocentric Frame.

Parameter	Units	Value	Reference
a_i , $i=d, b, h$	[pc]	3500, 0, 0	(1)
b_i , $i=d, b, h$	[pc]	250, 350, 24000	(1)
M_i , $i=d, b, h$	[$10^{10} M_\odot$]	7.91, 1.4, 69.8	(1)
Galactic center position (RA, Dec)	[hr/min/s, deg/'/'']	17 : 45 : 37.224, -28 : 56 : 10.23	(2)
Solar distance from center	[kpc]	8.3 ± 0.35	(3)
Solar height above galactic plane	[pc]	27 ± 4	(4)
Solar peculiar velocity (U,V,W)	[kms $^{-1}$]	$11.1^{+0.69}_{-0.75}$, $12.24^{+0.47}_{-0.47}$, $7.25^{+0.37}_{-0.36}$	(5)
Circular velocity at solar radius	[kms $^{-1}$]	218 ± 6	(6)

NOTE—

References.(1) [Dauphole & Colin \(1995\)](#), (2) [Reid & Brunthaler \(2004\)](#), (3) [Gillessen et al. \(2009\)](#), (4) [Chen et al. \(2001\)](#), (5) [Schönrich et al. \(2010\)](#), (6) [Bovy \(2015\)](#).

2.1.1. Initial Conditions of ‘Oumuamua

The initial conditions of ‘Oumuamua at -3000 years are provided by [Bailer-Jones et al. \(2018\)](#). Throughout our determination of possible source regions of ‘Oumuamua in section 3.3, we characterize the uncertainty in their $2k=2$ solution for ‘Oumuamua’s orbit by generating 100 clones of ‘Oumuamua, each having an initial velocity randomly sampled from a distribution whose mean and standard deviations are recorded in [Bailer-Jones et al. \(2018\)](#). We do the same with our own determination of the state of ‘Oumuamua at $-10\,000$ years in the past, but the initial positions as well as the velocities are randomly sampled. Our clones are derived from the JPL orbit and covariance matrix² and back-integrated with the RADAU ([Everhart 1985](#)) algorithm with a time step of -1 day and an error tolerance of 10^{-12} , under the influence of the Sun and the planets. The $2k=2$ and our own solution are recorded in Table 2.

2.2. Integrators

We will report on two types of simulations here. The first involves the back-integration of ‘Oumuamua alone within the potential of our Galaxy under the effect of disk heating. This is to examine the effects of gravitational scattering on the asteroid’s past trajectory and assess how far back we can expect to go reliably. These simulations are performed with the RADAU ([Everhart 1985](#)) integrator in Cartesian coordinates with a time step of 1000 years and an error tolerance of 10^{-12} .

² <https://ssd.jpl.nasa.gov/sbdb.cgi>, retrieved 18 June 2019

Table 2. Initial conditions of ‘Oumuamua in the ICRS frame. The 2k=2 solution provided by Bailer-Jones et al. (2018) and our own determination are supplied here at different times. Positions are recorded in Right Ascension (α), Declination (δ), and distance (d), and the radial velocity is recorded as (v_r). Each coordinate’s 1- σ uncertainties are provided where possible. The 2k=2 solution has no accompanying positional uncertainties in Bailer-Jones et al. (2018).

Solution	Time	α	σ_α	δ	σ_δ	d	σ_d	v_r	σ_{v_r}
	[yr]	[deg]	[deg]	[deg]	[deg]	[AU]	[AU]	[km s ⁻¹]	[km s ⁻¹]
2k=2	−3000	279.4752		33.8595		28000.0000		−26.4204	0.001145
This work	−10000	279.5588	0.002746	33.8795	0.001484	55674.1550	2.0930	−26.4052	0.003111

NOTE—2k=2 is taken from Bailer-Jones et al. (2018).

The second set of simulations computes the back-trajectory of ‘Oumuamua and many stars and other systems, and includes the galactic potential but no random impulses. These simulations are designed to examine close encounters between the nominal paths of known galactic objects and ‘Oumuamua to assess possible origin points for this asteroid. For these simulations, SciPy’s `solve_ivp` RK45 implementation of a mixed fourth/fifth order Runge-Kutta integrator method is used in numerically integrating the motion of the objects. This method is called to repeatedly integrate the positions and speeds of objects every 10 000 years. In each 10 000 year interval the distance to ‘Oumuamua is checked before integrating backward another 10 000 years. The time step it takes over each 10 000 year interval is set automatically by the solver. The error tolerances are the default values, 10^{-6} in absolute tolerance and 10^{-3} in relative tolerance. The integrations are carried out in cylindrical coordinates according to the equations of motion in a cylindrical system under a potential,

$$\ddot{R} = -\frac{\partial\Phi}{\partial R} + R\dot{\theta}^2, \quad (3)$$

$$\ddot{\theta} = -\frac{1}{R^2} \frac{\partial\Phi}{\partial\theta} - 2\frac{\dot{R}\dot{\theta}}{R}, \quad (4)$$

$$\ddot{z} = -\frac{\partial\Phi}{\partial z}. \quad (5)$$

2.3. Disk heating models

For simulations that include the effects of disk heating, that effect will be modelled as a series of random kicks to the velocity of each of an ensemble of particles (‘clones’) with similar initial conditions as we integrate them backwards within the Galactic potential. The increasing dispersion in the positions and velocities of this ensemble as we go further into the past will provide a measure of how well we can hope to locate the true position of ‘Oumuamua at that time.

Velocity kicks of 10 km s^{-1} are applied independently to each clone at random times according to a Poisson process with characteristic time scale of 200 Myr; these have been found to provide the best fit to the local galactic age-velocity relation (Wielen 1977; Mihalas & Binney 1981). Because the precise nature of the deflection depends on the details of the encounters, which are not known, we apply the kicks in three ways to examine the envelope of possible outcomes.

1. A velocity kick of 10 km s^{-1} applied in a random direction on the sphere (‘fixed kick’)
2. A velocity kick drawn from a three dimensional Maxwell-Boltzmann distribution with a most probable speed of 10 km s^{-1} (‘Maxwellian’)
3. A deflection of the velocity vector without changing its magnitude (‘Maxwellian deflection’). In this case, kicks drawn from a one-dimensional Maxwell-Boltzmann distribution with most probable speed of 10 km s^{-1} are applied along two orthogonal directions perpendicular to the velocity, which is then renormalized to its original length. This corresponds to the rotation of the velocity vector expected from long-range ‘dispersion-dominated’ encounters (Binney & Tremaine 1987).

3. RESULTS AND DISCUSSION

3.1. Integrations with disk heating: past trajectory

The increase in the dispersion, as measured by the standard deviation, of the positions and velocities of our clones of ‘Oumuamua are presented in Fig 1. Two sets of clones are examined, based on our own determination of the pre-arrival velocity of ‘Oumuamua and the 2k=2 solution from Bailer-Jones et al. (2018), which is based on the Micheli et al. (2018) solution with pure radial acceleration proportional to heliocentric distance r^{-2} . As we go back in time, the

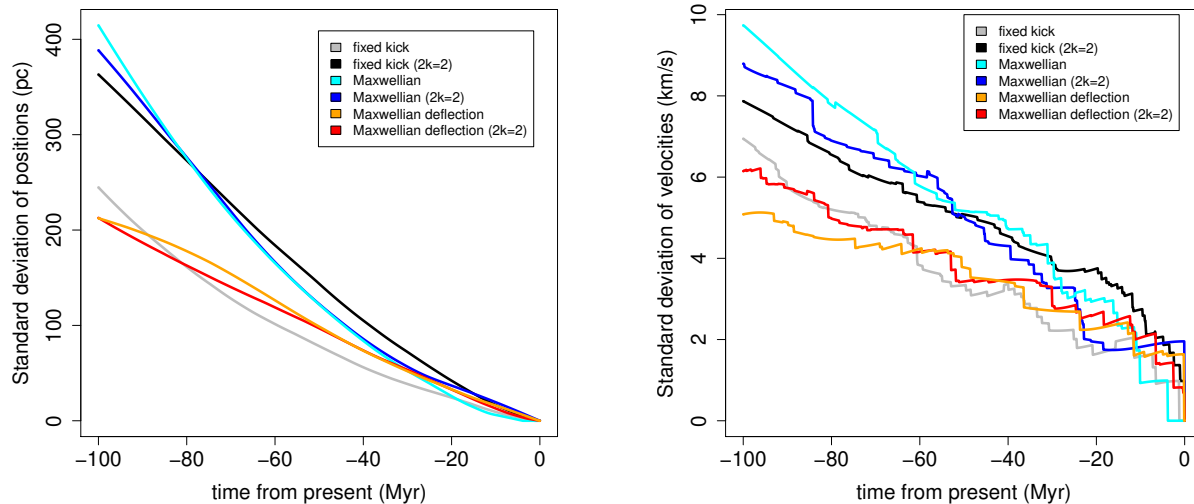


Figure 1. The standard deviation of the position and velocity of clones of ‘Oumuamua integrated backwards within the Galaxy.

dispersion of the clones grows, reaching up to 15 pc and 2 km s^{-1} at 10 Myr, 100pc and 5 km s^{-1} at -50 Myr, and 400 pc and 10 km s^{-1} at -100 Myr depending on the model chosen. Recall that at this point we are not integrating any stars or other objects within our Galaxy; we are purely assessing the uncertainty in the position and velocity of ‘Oumuamua.

As we investigate possible origin systems for ‘Oumuamua, Fig 1 will serve as a guide as to how close an encounter and how low a relative speed constitute an interesting encounter in terms of a possible origin. Though we cannot know what impulses ‘Oumuamua has undergone during its past, we can state that the true position and velocity of ‘Oumuamua at some specific time in the past is most likely within the dispersion given by our models from its nominal trajectory. As a result, the source system of ‘Oumuamua is as well, and we will use this to try to constrain its location of origin. Thus Fig. 1 provides us with a ‘sphere of interest’ around ‘Oumuamua at any point in time.

It is worth noting that the growing ‘sphere of interest’ around ‘Oumuamua as we move into the past creates a clear danger that mere coincidence might provide an erroneous good match with a candidate system of origin. A close encounter between ‘Oumuamua and a potential source region within our Galaxy 50 Myr ago at a relative speed of 5 km s^{-1} and a distance of 100 pc would provide roughly as good a match as one 10 Myr ago at 15 pc and 2 km s^{-1} . We will try to avoid this trap by carefully discussing the context of any interesting origin candidates found, and in any case at least, Fig. 1 provides us with a quantitative measure of the degree of danger at any point.

3.2. Integrations with impulses: distance to ‘Oumuamua’s origin point

The end states of our ensemble of the previous section provide a probability distribution outlining our uncertainty in the location of ‘Oumuamua up to 100 Myr ago. If that young age is correct, and ‘Oumuamua was ejected at a low relative velocity, then the origin system of ‘Oumuamua was, from Fig 1, within about 400 pc of our mean end state 100 Myr ago. In order to assess where that origin point might be currently, we will use those afore-mentioned end states as proxies for the origin point’s location 100 Myr ago, and integrate them forward to the present day. Such a use of ‘Oumuamua’s end states to model the rough dynamics of its origin system will be correct as long as 1) ‘Oumuamua and its point of origin were co-located at ‘Oumuamua’s time of origin (satisfied by definition) and 2) they were travelling at low relative velocity at the time of ejection (which is the most likely case for most ejection mechanisms).

Figure 2 shows the results of these forward simulations. The position and velocity dispersions start with decreasing trends as one moves left to right as the previously expanding cone of ‘Oumuamua clones initially contracts. Eventually, the impulses due to disk heating cause enough scatter for them to begin diverging again, which takes about 40 Myr. The standard deviation (1-sigma) in position and velocity at the righthand side of both panels of Fig. 2 imply that the origin system of ‘Oumuamua is at this moment within 300-600 pc and moving 11-13 kms^{-1} with respect to the LSR. At the 2-sigma or 95% confidence level, ‘Oumuamua’s origin system should be within 1.2 kpc of Earth, within the local Orion Arm, and thus relatively easily accessible to Earth-based study. There are a number of nearby star-forming regions, plausible sources of asteroids, in Perseus, Orion, Taurus and Ophiuchus which we will assess as possible origin points in the next sections.

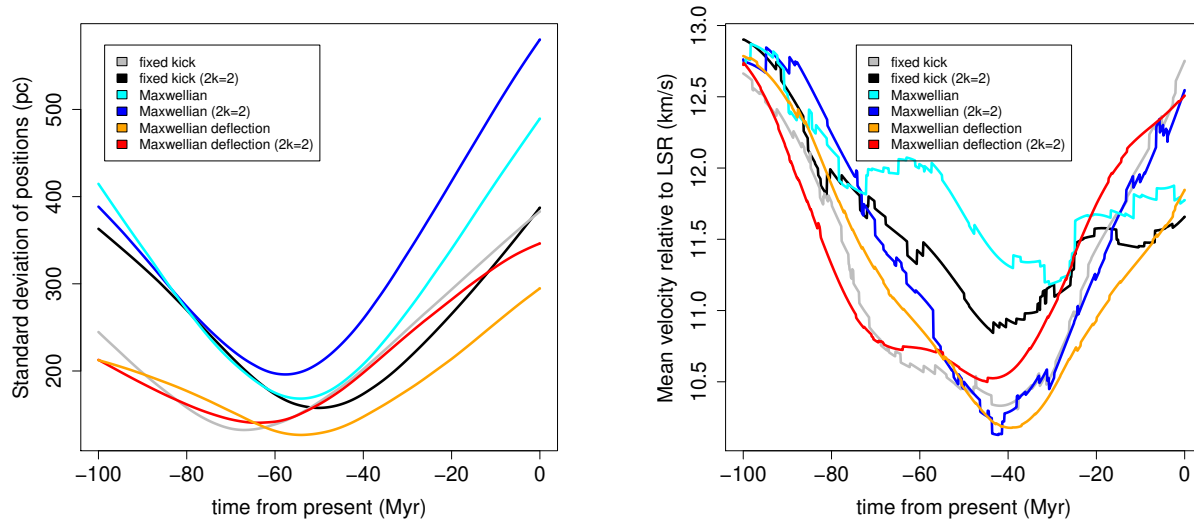


Figure 2. The dispersion of the modelled origin system positions (relative to the mean at a given time) and velocity (measured with respect to the Local Standard of Rest at their mean position at a given time) integrated forwards to the current time within the Galaxy. Note that though the left-hand panel shows the same quantity as Fig. 1, the right-hand panel is different and shows here instead the mean velocity of our modelled origin systems with respect to the LSR.

3.3. Integrations without impulses: close encounters

3.3.1. Extending previous results

A number of efforts have been made to understand ‘Oumuamua in the context of the close galactic neighbourhood, including but not limited to the work of Bailer-Jones et al. (2018), Zuluaga et al. (2018), Feng & Jones (2018), Portegies Zwart et al. (2018), Dybczyński & Królikowska (2018), Mamajek (2017), Zhang (2018), Gaidos et al. (2017), Gaidos (2018), and Eubanks (2019). Here we extend these by providing a uniform treatment of all stars in the Gaia DR2 catalog, the Catalog of Suspected Nearby Young Stars (Riedel et al. 2018), the compilation of bonafide members of kinematic groups in Gagné et al. (2018), and SIMBAD, under an understanding of the limitations imposed by disk heating, as derived in the earlier sections.

As other authors have pointed out, given that ‘Oumuamua is likely young, it may have come from one of the many sources of young stars nearby in the galaxy. Young stars are most frequently observed as members of star-forming regions (SFRs), open clusters, and moving groups. Some of the closest SFRs include Scorpius-Centaurus (Sco-Cen) at $d \sim 118\text{-}145$ pc (Preibisch & Mamajek 2008), Taurus-Auriga at $d \sim 140$ pc (Galli et al. 2018), Chamaeleon I, II, and III at $d \sim 180\text{-}200$ pc (Voinin et al. 2018), and the Lupus clouds at $d \sim 110\text{-}190$ (Galli et al. 2013).

Many young stars within 100 pc of the sun are categorized into members of open clusters and nearby young moving groups (NYMGs) (Riedel et al. 2017). Clusters and moving groups are thought to be born in molecular clouds, and slowly disperse over millions of years due to feedback between the stars and material left over from the star formation process (Wright & Mamajek 2018). Before dispersing into the galaxy, the young stars form an *association*, a group of stars which share similar kinematics. A number of kinematically-related young stars have been identified in the

past few decades, and the associations and moving groups they constitute have been continuously redefined with the advent of better astrometric surveys. The most up-to-date classifications define three open clusters within 100 pc of the sun (Coma Ber, Hyades, and η Cha), and ten NYMGs (Riedel et al. 2017).

Riedel et al. (2017) provide a thorough overview of the current understanding of the open clusters and moving groups within 100 pc of the sun. Moving groups are distinguished from open clusters by the fact that they are loose and gravitationally unbound. Moving groups are older than SFRs, but much closer. All stars contained within a moving group or open cluster are thought to originate from the same star forming event, so share the same position in space at time of formation, as well as the same age, composition, and because they are young, the same galactic space motion as their natal gas clouds (Riedel et al. 2017).

Of the previous studies which mention moving groups or kinematic associations in the context of ‘Oumuamua (such as Feng & Jones (2018), Gaidos et al. (2017), Gaidos (2018), or Eubanks (2019)), Feng & Jones (2018) include integrations of the motion of ‘Oumuamua and stars in the Pleiades association, Gaidos (2018) present integrations of ‘Oumuamua along with the mean positions and velocities of many of the nearest moving groups (incl. the Carina and Columba Associations), while Gaidos et al. (2017) and Eubanks (2019) only consider the UVW kinematics of the moving groups with respect to ‘Oumuamua without integrations. We extend these results by explicitly integrating the known and suspected members of the NYMGs and open clusters within 150 pc, along with other stars such as YSOs which belong to the nearest SFRs. Although integrating the mean positions and velocities of the moving groups was found not to reveal any close encounters between them and ‘Oumuamua in the past (Gaidos 2018), we find many individual slow encounters with members of various groups which are close enough to plausibly interact with ‘Oumuamua if dynamical heating is accounted for. The NYMGs which have the most such encounters are Carina, Columba, and TW Hydra. The stars in Carina and Columba in particular minimize their distance to ‘Oumuamua roughly during the moving groups’ formation epoch, ~ 30 -45 Myr in the past (Riedel et al. (2017) and references therein). Since we expect bodies like ‘Oumuamua to be ejected in large numbers during the stages of planet formation, the low encounter distances and velocities observed with respect to Carina/Columba association just as it is forming make it a particularly attractive candidate source region.

We draw stars which are bonafide or suspected members of each moving group from two sources. The principle source we use is the Catalog of Suspected Nearby Young Stars as supplied in Riedel et al. (2018). This catalog is intended as ‘a single resource for studying the individual and ensemble properties of young stars’ (Riedel et al. 2017). It has been compiled from careful scrutiny of numerous publications of moving group candidates, and contains basic information for any star system within 100 pc that has ever been reported as young. Of the many properties of the young stars compiled, their astrometry and moving group membership are recorded. We use each star’s *GROUP1* entry in the catalog to categorize it into each NYMG, and regard the stars with positive *Bonafide* entries as high-confidence members. The catalog supplies astrometry for 4 727 stars with *GROUP1* classifications. For additional data, we supplement with bonafide members compiled from the literature in Gagné et al. (2018) (Table 5). The populations of suspected and bonafide moving group members recorded in the Catalog of Suspected Nearby Young Stars is provided in Table 3, while the number of bonafide stars in each group recorded in Gagné et al. (2018) are given in Table 4.

We further supplement these data with all stars from SIMBAD with full astrometric solutions recorded, classified by object type (Young Stellar Objects, white and brown dwarfs, low-mass stars, etc.). We also use all Gaia Data Release 2 stars with full astrometric solutions recorded. Although many of the Gaia and SIMBAD stars have previously been considered (Bailer-Jones et al. (2018), Dybczyński & Królikowska (2018), Zuluaga et al. (2018), Feng & Jones (2018), Portegies Zwart et al. (2018), etc.), we check our results against these previous studies’ and extend them by looking specifically for YSOs in SFRs, as well as stars in nebulae and other extended objects.

In addition to integrating 100 clones of ‘Oumuamua from the $2k=2$ solution, we sample the astrometric coordinates of the stars in our data set from Gaussian distributions with means and standard deviations given by the nominal values and their corresponding uncertainties. Altogether 100 clones of ‘Oumuamua interact with 100 clones of each star in each of our integrations to provide distributions in the relative speeds and distances at the time of closest approach. We use the $2k=2$ solution for consistency with previous studies. However, we find that in general the uncertainty in ‘Oumuamua’s initial conditions is dwarfed by the uncertainties in the astrometric data used in our integrations; our results are not strongly sensitive to whether the $2k=2$ or our own clones of ‘Oumuamua are used. The results differ generally at the $\sim 100 \text{ ms}^{-1}$ level in speed, and at the ~ 0.1 pc level in median encounter distance.

Although the Catalog of Suspected Nearby Young Stars may be considered complete up to January 2015 (Riedel et al. 2017), newer astrometry exists for many of the stars due to Gaia. However, no database has been compiled that

contains the same membership data as the Catalog of Young Stars but with the newest astrometry. We checked our results by re-integrating each star in Table 6 with all available Gaia measurements (excluding Gaia radial velocities with higher uncertainties than those recorded in the Catalog). We find significantly different results for a minority of stars; 2 of the 16 Carina stars were found not to pass close enough to ‘Oumuamua, and one bonafide member, HD 83096, had an encounter time of 16.53 Myr as opposed to the 31.02 Myr recorded in Table 6. Nevertheless, the average time of encounter between the 14 Carina stars was -31.82 Myr, and between the 4 Bonafide stars it was -28.62 Myr. The average time of closest approach between all 21 Columba stars in Table 6 was found to be -26.00 Myr in the past, while the average encounter time between the 9 bonafide members was -24.73 Myr. The results are therefore only weakly sensitive to whether the Gaia astrometry or that contained in the Catalog of Young Stars is used. An illustration of the approach of ‘Oumuamua to Earth is shown in Animated Figure 3.

Table 3. Suspected and bonafide members of moving groups from Riedel et al. (2017) considered in this work. Each total is the number of stars in the group with radial velocity data recorded. Group classification is based on each star’s *GROUP1* entry in the catalog.

Group	No. total	No. Bonafide
Columba	103	15
Carina	38	3
TW Hydra	77	17
AB Dor	338	34
Pleiades/Local Association	78	16
Coma Ber	54	33
Tucana-Horologium	311	32
Ursa Major	271	0
η Cha	15	0
Hercules-Lyra	53	2
Beta Pic	216	28
IC 2391	37	0
Hyades	12	0

3.3.2. Candidate Regions

The systems which move at appropriately low speed and whose distances from ‘Oumuamua are within the bounds imposed by disk heating at the time of encounter are summarized in Table 6, along with each system’s object type, time of encounter, and membership in any SFR or moving group. Bonafide members of moving groups are labelled with an additional ‘*’ beside their identifier. The table does not follow any inherent ranking of the candidates.

The most interesting candidate source regions are those with the most encounters consistent with a low relative speed ($\lesssim 5 \text{ kms}^{-1}$), encounter distances within the bounds imposed by disk heating, and those for which the closest encounters occur at times that are allowed considering the age of the group, SFR, or individual star. The most interesting source regions we find are the Carina and Columba moving groups. ‘Oumuamua has its closest encounter to multiple members of these groups at $< 5 \text{ kms}^{-1}$, at median times of -32.89 Myr and -25.63 Myr, respectively, close to the 30-45 Myr age range of these systems (Riedel et al. 2017), when they can be expected to be ejecting the most material. Another strong case can be made for the Lupus SFR. We find 4 encounters with YSOs at $5 - 7 \text{ kms}^{-1}$. Two are members constituting the Lupus core moving group (Galli et al. 2013), and 2 have been identified as members of the Lupus population of weakline T-Tau stars (Galli et al. 2013), the ages of which have been found to be considerably older than the Lupus classical T-Tau population (Makarov 2007). To explain this spread in ages it has been suggested that there may have been multiple bursts of star formation events in Lupus (Makarov 2007) and this would roughly align with the epoch of ‘Oumuamua’s closest approach to these two stars. We find two promising

Table 4. Bonafide Members of Moving Groups From Gagné et al. (2018) Considered in This Work

Group	No. Total (=Bonafide)
Columba	19
Carina	5
TW Hydra	22
AB Dor	47
Pleiades/Local Association	187
Coma Ber	41
Tucana-Horologium	31
η Cha	16
Beta Pic	47
IC 2391	10
Hyades	165
Carina-Near	18
Corona Australis	13
ϵ Cha	23
IC 2602	10
Lower Centaurus Crux	81
Octans	10
Platais 8	11
ρ Ophiuchi	180
Taurus	121
32 Orionis	31
Upper Centarus Lupus	102
Upper CrA	23
Ursa Major cluster	7
χ^1	11

encounters with T-Tau stars, one possibly associated with the Orion Cluster, moving at just 3.84 kms^{-1} relative to ‘Oumuamua. Additionally, GJ 1167 A is a young m dwarf passing within 3.9 pc, 2.4 Myr ago, at 4.9 kms^{-1} . Other YSOs with plausible but less compelling encounters have been identified belonging to the Taurus-Auriga SFR. Two of these encounters are at times when the SFR may have been active. A detailed analysis of our results is provided below.

- **Lupus SFR:** HD 143978 is one of 4 YSOs in Lupus we identify as plausible candidates. It moves at 5.34 kms^{-1} ($4.25\text{-}6.35 \text{ kms}^{-1}$ in the 5th to 95th percentiles), and encounters ‘Oumuamua 18.87 Myr in the past, at a distance of 11.78 pc (8.66-14.75 in the 5th to 95th percentiles). Disk heating implies a spread in distance between clones of ‘Oumuamua of at least ~ 20 pc 18 Myr in the past. HD 143978 is a putative member of the Lupus dark cloud complex, one of the nearest SFRs (Galli et al. 2013). HD 143978’s galactic coordinates ($l=339.10^\circ$, $b=9.96^\circ$) place it in the *on-cloud* component of the Lupus SFR as defined in Galli et al. (2013), a population of young stars in the immediate vicinity of the Lupus molecular clouds. More specifically, its coordinates indicate that it is a member of the Lupus 3 star forming cloud (see Figures 3 or 15 in Galli et al. (2013)). Although its geometric distance ($d\sim 97$ pc) does not align with the average distance to Lupus 3 ($d_{avg}=185^{+11}_{-10}$ pc according to Galli et al. (2013)), Galli et al. (2013) include stars with parallaxes in the range 10-12 mas in defining the membership of Lupus 3 (see their Figure 16). Furthermore, Galli et al. (2013) in their Table 7 exclude it from the population of Lupus stars with doubtful membership status (in Lupus or Upper Centaurus-Lupus) in the literature. We additionally note that its updated parallax measurement from Gaia DR2 places it closer to the Lupus clouds

(whose average distances range from ~ 140 - 200 pc according to Galli et al. (2013)) than the measurement from TYCHO2 used in Galli et al. (2013) (TYCHO2 records its parallax as 11.6 ± 2.6 mas, placing it ~ 86 pc away, whereas Gaia DR2 measures 10.28 ± 0.036 mas, placing it ~ 97 pc away).

RX J1531.3-3329 has been listed as one of 19 stars which constitute the Lupus core moving group (Galli et al. 2013). Its coordinates ($l=337.33^\circ$, $b=18.49^\circ$) place it possibly in the Lupus 1 dark cloud or in the *off-cloud* population according to Figures 3 and 15 in Galli et al. (2013). Its distance to ‘Oumuamua minimizes at the maximum simulation time however, and is quite large ($d_{enc}^{med} = 91.74$ pc). RX J1531.3-3329’s slow speed of 5.19 kms^{-1} (5.02 - 5.40 kms^{-1} in the 5th and 95th percentiles) indicates that the Lupus moving group moves relatively slowly with respect to ‘Oumuamua.

A weak-line T-Tau star in the Lupus SFR, 2MASS J15480212-4004277, was found to pass within 48.19 pc (24.05 - 92.47 pc in the 5th and 95th percentiles), at 7.09 kms^{-1} (6.14 - 8.69 kms^{-1} in the 5th and 95th percentiles), 23.24 Myr in the past. These conditions were found using Gaia DR2 astrometry for everything but radial velocity, which was taken from observations recorded in Galli et al. (2013) (Table 4, where $v_r = 2.07 \pm 0.35$ kms^{-1}). Using the Gaia DR2 radial velocity produces an encounter with $d_{enc}^{med} = 70.84$ pc (28.26 - 136.95 pc in the 5th and 95th percentiles), 6.95 kms^{-1} (4.57 - 13.00 kms^{-1} in the 5th and 95th percentiles), 14.97 Myr ago. The Gaia radial velocity however is highly uncertain ($\sigma_v = 4.2$ kms^{-1}), so this YSO remains inconclusive. Based on its parallax, it likely belongs to the off-cloud component of the Lupus weak-line T-Tau stars (Galli et al. 2013).

2MASS J16081096-3910459 is another weak-line T-Tau star in the Lupus region (Makarov (2007), Galli et al. (2013)). This passes within 87.35 pc (77.18 - 99.87 pc in the 5th and 95th percentiles), at 5.98 kms^{-1} (5.56 - 6.96 kms^{-1} in the 5th and 95th percentiles), 34.03 Myr ago. This star currently lies ~ 149 pc away. It has also been included as a defining member of the Lupus core moving group (Galli et al. 2013). Its coordinates place it either in the Lupus off-cloud weak-line T-Tau star population, or possibly in Lupus 3.

While the exact depths and spatial distribution of the Lupus clouds is not fully understood (Galli et al. 2013), given the large depth of the Lupus SFR (individual distances to association members range from ~ 110 - 190 pc according to Galli et al. (2013), while Lombardi et al. (2008) independently estimate the depth of Lupus to be 51_{-35}^{61} pc), these encounters suggest ‘Oumuamua could have interacted with the Lupus 3 or 1 clouds, or perhaps the off-cloud population in the immediate vicinity of the SFR. The age of the SFR has been estimated to be 3 Myr (Hughes et al. 1994), but newer analyses have found a considerable spread in ages of the stars in Lupus (eg. Makarov (2007)). The population of weak-line T-Tau stars were found to be older, several of them being ~ 25 - 30 Myr old, while half the classical T-Tau stars were found to be less than 1 Myr old (see their Figure 4). At least two of our Lupus candidates are indeed weak-line T-Tau stars. HD 143978 may be a member of the younger population, owing to it possibly belonging to the Lupus 3 filament, which was found to harbour a sizeable number of young T-Tau stars (Makarov 2007). Makarov (2007) note that a possible explanation for the large spread in stellar age is multiple, separate star formation episodes. Thus, ‘Oumuamua may have been close enough to this cloud to have been ejected at the time of one of these episodes.

- **Carina and Columba moving groups:** A number of bonafide or suspected members of the Carina and Columba moving groups are recorded in Table 6. Of the 16 stars associated with Carina in Table 6, 4 are bonafide members according to Riedel et al. (2017) and Gagné et al. (2018) (HD 49855, HD 55279, HD 83096 a and b, and V479 Car). HD 83906 a and b make up one multiple star system. Their encounter conditions are similar, so we take the system’s encounter with ‘Oumuamua to be that of HD 83096 a’s. There are in total 6 unique bonafide members of Carina in our initial data set. The age of Carina has been estimated between 30 and 45 Myr (see Riedel et al. (2017) and references therein). The median encounter time between the bonafide Carina stars is -31.46 Myr, and for all Carina stars in Table 6 the median encounter time is -32.89 Myr. ‘Oumuamua minimizes its distance from a number ($\sim 40\%$) of Carina stars, (15 out of 41 total), *4 of which are bonafide members out of 6 total*, at the minimum age of the group. This suggests ‘Oumuamua may have had an encounter with the group at a very early stage in its history, either during the initial star-forming epoch or after, as the young stars gradually dispersed.

One star in particular in Carina, GJ 1167 A, passes within 3.94 pc (2.41 - 11.64 pc in the 5th and 95th percentiles), at 4.90 kms^{-1} (2.0 - 8.06 kms^{-1} in the 5th and 95th percentiles), 2.37 Myr ago. The dispersion due to disk heating

at 2.37 Myr is ~ 2.4 pc, so assuming ‘Oumuamua was ejected 2 pc away from its origin star, this encounter fits within these bounds. It has an exceptionally low speed. GJ 1167 is a young m dwarf, currently ~ 12 pc away.

Of the 21 stars associated with Columba in Table 6, 9 are bonafide members; HD 40216, HD 38206, HD 30447, HR 8799, HIP 1134, HD 32372, HD 32309, HD 37484, and 2MASS J05184616-2756457. There are in total 29 unique bonafide Columba stars in our initial data set. The median time of encounter between the 9 bonafide stars is 23.85 Myr ago, while the median encounter time between all Columba stars in Table 6 is 25.63 Myr. The estimated age of the Columba group is between 30-42 Myr in the past (Riedel et al. 2017). ‘Oumuamua therefore minimizes its distance to a lesser number ($\sim 18\%$) of Columba stars, slightly before the group’s minimum age.

- **Taurus-Auriga SFR:** V1319 Tau moves at 6.91 kms^{-1} ($6.82\text{-}7.06 \text{ kms}^{-1}$ in the 5th and 95th percentiles), and encounters ‘Oumuamua 28.53 Myr in the past, at a distance of 21.79 pc (18.81-25.18 pc in the 5th and 95th percentiles). Its astrometry is taken from its SIMBAD entry, where all measurements but its radial velocity are from Gaia DR2. The SIMBAD record for radial velocity is taken from Nguyen et al. (2012). The Gaia DR2 velocity has much larger uncertainty ($\sigma_{v_r} = 6.36 \text{ kms}^{-1}$), and produces a much larger spread in encounter conditions. It has an estimated age of $13.00^{+6.50}_{-3.30}$ Myr (Davies et al. 2014), though could be as large as 20 Myr (Hambálek et al. 2019). It has been recorded as a member of the Taurus-Auriga SFR in previous studies (Kraus et al. 2017), but is not included in the recent census provided by Luhman (2018), possibly owing to its updated Gaia DR2 parallax placing it slightly outside the SFR. Although the canonical distance of the Taurus clouds at $d \sim 140$ pc away (Galli et al. 2018) is farther than V1319’s geometric distance at ~ 112 pc, the region’s depth has been estimated to be at least 20 pc (Kenyon et al. (1994), Torres et al. (2007), Torres et al. (2012)). Furthermore, Bertout & Genova (2006) found that although the population of classical T Tau stars resides 126-173 pc away, weak line T Tau stars surround the molecular clouds between 106-256 pc. V1319 may therefore reside in the immediate surroundings of the clouds. Kraus et al. (2017) record it as a ‘Class III’ (disk-free) candidate member of the Taurus-Auriga ecosystem.

2MASS J03190760+3934105 is a T-Tau star, which passes within 16.45 pc (4.85-43.65 pc in the 5th and 95th percentiles), at 6.11 kms^{-1} ($5.33\text{-}6.61 \text{ kms}^{-1}$ in the 5th and 95th percentiles), 29.59 Myr in the past. At $d \sim 143$ pc, it has been suggested to be an outlying member of the Taurus-Auriga SFR, situated on the border of the molecular clouds (Li & Hu 1998). Comparing its Right Ascension and Declination to the spatial distribution of Taurus stars provided in Kraus et al. (2017) (Figure 8) indicates that this star is likely situated on the outskirts of the main SFR. However, no newer studies seem to mention a connection between this star and the Taurus SFR, so its classification remains inconclusive.

HD 30171 is a well-known T-Tau star, passing within 46.05 pc (15.96-104.13 pc in the 5th and 95th percentiles), at 8.01 kms^{-1} ($6.89\text{-}9.39 \text{ kms}^{-1}$ in the 5th and 95th percentiles), 43.81 Myr ago. The age of this star has been estimated to be 2-4 Myr (Hambálek et al. 2019), ruling this out as a possible origin.

V1267 Tau is a T-Tau star which has been classified as in the immediate surroundings of the Taurus-Auriga clouds (Broeg et al. 2006). It passes within 40.55 pc (22.89-82.42 pc in the 5th and 95th percentiles), at 7.43 kms^{-1} ($6.8\text{-}107.83 \text{ kms}^{-1}$ in the 5th and 95th percentiles), 49 Myr ago.

It has been suggested that Taurus-Auriga has been producing stars for at least 10 Myr (Palla & Stahler 2002). These same authors identify multiple stars in Taurus-Auriga with ages ~ 20 Myr. Some of the older encounters with Taurus-Auriga stars are therefore too far in the past, but the encounters at 28 Myr and 29 Myr are perhaps not ruled out by these findings. These encounters indicate that ‘Oumuamua could have interacted with the Taurus-Auriga molecular clouds, or possibly with the components immediately surrounding the SFR.

- **Chameleon SFR:** Sz 46N lies in the Chamaeleon II dark cloud, one of three star-forming clouds in the Chamaeleon system (Alcalá et al. 2008). Chamaeleon II lies 178 ± 18 pc away (Alcalá et al. 2008). Sz 46N encounters ‘Oumuamua at a distance of 79.83 pc (48.90-138.60 pc in the 5th to 95th percentiles), 41.89 Myr in the past, moving at 7.02 kms^{-1} ($6.49\text{-}8.26 \text{ kms}^{-1}$ in the 5th and 95th percentiles). We find two other young stars belonging to the Cha II cloud; Hn 23 at 95.08 pc (83.23-106.12 pc in the 5th to 95th percentiles), 45.45 Myr ago, at 6.83 kms^{-1} ($6.69\text{-}6.99 \text{ kms}^{-1}$ in the 5th and 95th percentiles), and CM Cha at 85.38 pc (68.48-127.98 pc in the 5th and 95th percentiles), 44.20 Myr in the past, at 7.50 kms^{-1} ($6.95\text{-}9.00 \text{ kms}^{-1}$ in the 5th and 95th percentiles). Chamaeleon II has an estimated age of 4 ± 2 Myr (Spezzi et al. 2008). The encounter times for these YSOs are much longer than this, indicating that the Cha II region is unlikely to have interacted with

‘Oumuamua. A less likely scenario could be that ‘Oumuamua interacted with the primordial SFR in which Cha II was born.

Hen 3-545, which passes within 69.82 pc, (53.57-81.21 pc in the 5th and 95th percentiles), at 7.40 km s^{-1} ($7.27\text{-}7.59 \text{ km s}^{-1}$ in the 5th and 95th percentiles), 46.81 Myr ago, is a member of the Chamaeleon I star-forming region (Mulders et al. 2017), the most active center of star formation in the Chamaeleon cloud complex encompassing Cha I, II, and III (Reipurth 2008). 2MASS J11054153-7754441 is also a member of the Cha I cloud, passing within 69.37 pc (44.58-91.50 pc in the 5th and 95th percentiles), at 8.17 km s^{-1} ($7.89\text{-}8.41 \text{ km s}^{-1}$ in the 5th and 95th percentiles), 29.75 Myr ago. The age of the Cha I cloud has been estimated to be ~ 2 Myr (Reipurth 2008). The Cha I region is, similarly to Cha II, unlikely to be the origin of ‘Oumuamua due to its very young age relative to its time of closest approach to ‘Oumuamua.

In general, the relative speeds of the candidates in the Taurus-Auriga and Chamaeleon SFRs are higher than those from the Lupus SFR.

- **Scorpius Centaurus SFR:** CPD-53 5235 is a pre-main sequence star located in the Scorpius-Centaurus region (Song et al. 2012). It passes within 77.29 pc (57.99-102.57 pc in the 5th and 95th percentiles), at 4.32 km s^{-1} ($4.09\text{-}5.16 \text{ km s}^{-1}$ in the 5th and 95th percentiles), 29.41 Myr ago. The age of the subregions of Sco-Cen have been estimated to be 11 ± 2 Myr for Upper Scorpius, 16 Myr for Upper Centaurus-Lupus, and 17 Myr for Lower Centaurus-Crux (Pecaut et al. 2012). Given the discrepancy in ages, this star also appears unlikely to be the home of ‘Oumuamua.
- **TW Hya group:** TYC 8083-45-5 is a bonafide member of the TW Hydra group, and is the only bonafide member of that group we identify in Table 6. Of the more than 70 suspected or bonafide members of TW Hydra in our data set, only 3 pass within the distance bounds imposed by this study. This seems to rule out an origin in the TW Hydra group.
- **Pleiades/Local Association:** In light of the results of Feng & Jones (2018), it is perhaps unsurprising that 2 encounters at speeds $\sim 4\text{-}10 \text{ km s}^{-1}$ and distances $\sim 2\text{-}4$ pc, and 3 encounters at speeds $\sim 10\text{-}20 \text{ km s}^{-1}$ and distances $\sim 4\text{-}5$ pc, with 5 stars in the Pleiades/Local Association were found; there are 51 stars associated with this group with speeds less than 10 km s^{-1} , and 65 with speeds less than 20 km s^{-1} included in the Young Stars Catalog.

Given that there are multiple groups with more members than Carina and/or Columba (Pleiades, Tucana-Horologium, Ursa Major, and Beta Pictoris), it is encouraging that these 2 groups nevertheless produce the largest number of reasonable encounters (ie. with low-speed and distances within the disk heating bounds).

- **Other:** A number of individual stars with no association to moving groups or SFRs were also found. Because many of these have already been considered in previous works, they are not included in Table 6. We find very similar candidates from Gaia DR2 as those in Bailer-Jones et al. (2018), and also find similar candidates to those in Zuluaga et al. (2018) using SIMBAD data. Here we mention some of the stars which we deem most interesting and have not been thoroughly discussed already in the literature.

V391 Ori passes within 50.12 pc (43.24-62.10 pc in the 5th and 95th percentiles), 25.52 Myr ago, at 3.84 km s^{-1} ($3.77\text{-}4.01 \text{ km s}^{-1}$ in the 5th and 95th percentiles). V391 Ori has been classified as a weak-line T-Tau star associated with the Orion Nebula Cluster, and was found likely to possess an optically thick accretion disk (Szegedi-Elek et al. 2013). This star’s distance, $d \sim 100$ pc, places it some distance away from the nominal value for the Orion Nebula at $d \sim 400$ pc (Menten et al. 2007), so its encounter with ‘Oumuamua does not necessarily mean that ‘Oumuamua could have interacted with the clouds of Orion.

BD+11 414 is a T-Tau star passing within 34.61 pc (7.34-89.40 pc in the 5th and 95th percentiles), at 7.73 km s^{-1} ($7.09\text{-}9.73 \text{ km s}^{-1}$ in the 5th and 95th percentiles), 20.29 Myr ago. Its age has been estimated to be ~ 65 Myr (Carpenter et al. 2009). Given the large errors in distance we are less confident that this is a good candidate, but it nevertheless has an appropriate age, along with low speed and median distance.

HD 189210 is a young sun-like star, observed by the Kepler mission (Fröhlich et al. 2012). Its age has been estimated to be 100-200 Myr, though the authors note that their analysis could not exclude an age as young as 50 Myr (Fröhlich et al. 2012). It encounters ‘Oumuamua at a distance of 82.86 pc (80.41-90.57 pc in the 5th and

95th percentiles), 49.99 Myr ago, moving at an exceptionally low speed of just 1.84 kms^{-1} ($1.69\text{-}2.51 \text{ kms}^{-1}$ in the 5th and 95th percentiles).

EGGR 268 is a member of the population of local white dwarfs (Holberg et al. (2002), Oswalt et al. (2016)), one of the few with radial velocity data recorded (although it is highly uncertain). The encounter occurs at 3.28 pc ($2.27\text{-}6.73$ pc in the 5th and 95th percentiles), 650 kyr ago, at 24.62 kms^{-1} ($11.93\text{-}37.01 \text{ kms}^{-1}$). Ejection speeds from white dwarf tidal disruption events of interstellar asteroids have been predicted to be $\sim 10\text{-}30 \text{ kms}^{-1}$ (Rafikov 2018). It is also a binary system with an M dwarf companion (Oswalt et al. 2016).

HD 24260 is also white dwarf Guo et al. (2015), passing within 59.28 pc ($33.59\text{-}106.68$ pc in the 5th and 95th percentiles), at 5.09 kms^{-1} ($4.42\text{-}5.67 \text{ kms}^{-1}$ in the 5th and 95th percentiles), 30 Myr ago. Given the expected ejection speed of white dwarfs discussed above, this is quite a low speed.

3.3.3. *The Origin of 2I/Borisov*

Using the same code and data sets we have also probed the origin of the second interstellar object discovered, comet 2I/Borisov (Guzik et al. 2019). The orbital elements of the comet were obtained from JPL on 2 October 2019 and back-integrated in the manner described in section 2.1.1. We find the Ursa Major group to have the slowest relative speed. The average encounter distance for the stars within the disk heating bounds is 15.65 pc, 133 kyr ago, at 26.10 kms^{-1} . Every other group had average encounter speeds higher than this, typically in the $30\text{-}40 \text{ kms}^{-1}$ range. Owing to the moving groups' high relative speeds and large distances of encounter, it seems unlikely that this comet comes from any of the nearest young moving groups or kinematic associations. The final stages of its approach to Earth is shown in Animated Figure 3.

Three stars in the Ursa Major group have plausible encounters with Borisov. GJ 4384 is a multiple star system which passes within 0.32 pc ($0.11\text{-}0.80$ pc in the 5th and 95th percentiles), at 19.15 kms^{-1} ($18.74\text{-}19.52 \text{ kms}^{-1}$ in the 5th and 95th percentiles), 1.46 Myr ago. EV Lac (Gaia DR2 1934263333784036736), a young M dwarf, has a very recent encounter at 0.97 pc ($0.96\text{-}0.97$ pc in the 5th and 95th percentiles), 27.44 kms^{-1} ($27.27\text{-}27.61 \text{ kms}^{-1}$ in the 5th and 95th percentiles), just 150 kyr ago. Lastly, GJ 102, also a flare star, passes within 1.98 pc ($1.09\text{-}5.27$ pc in the 5th and 95th percentiles), at 28.26 kms^{-1} ($13.43\text{-}44.94$ in the 5th and 95th percentiles), 273 kyr ago.

2MASS J03552337+1133437 is a brown dwarf, passing within 0.44 pc ($0.32\text{-}0.55$ pc in the 5th and 95th percentiles), 32.06 kms^{-1} ($31.49\text{-}32.46 \text{ kms}^{-1}$ in the 5th and 95th percentiles), 280 kyr in the past. This is a bonafide member of the AB Dor group (Gagné et al. 2018).

We find eight stars using Gaia DR2 astrometry which pass within 2 pc at speeds less than 30 kms^{-1} (including EV Lac). Gaia DR2 6223838830917236224 has the slowest speed at 13.25 kms^{-1} , 1.63 pc ($1.47\text{-}1.79$ pc in the 5th and 95th percentiles), 1.95 Myr ago. There are nine additional Gaia stars which pass within 2 pc at speeds between 30 and 40 kms^{-1} . The Gaia stars were only integrated backwards 10 Myr.

These candidates have been summarized Table 7, organized according to distance. There are more stars passing within 2 pc at speeds greater than 50 kms^{-1} , but due to their high speeds they have not been included in Table 7.

We do not find any YSOs or stars in SFRs.

Table 6. Plausible local galactic candidates of origin for ‘Oumuamua. Plausible systems of origin are listed along with the results of dynamical integrations for the distributions in relative speed and distance. Median times of encounter are also recorded. Along with main identifier, each system has its SIMBAD object type recorded. Membership of systems in star-forming regions (SFRs) or moving groups is also indicated. Bonafide members of moving groups have * beside their identifier; suspected members do not. Stars with (?) included in their *Region/Group* entries have ambiguous membership. These results were obtained using the 2k=2 solution for ‘Oumuamua as provided in Bailer-Jones et al. (2018). Astrometric data was taken from (Riedel et al. 2018) and SIMBAD. The results do not change appreciably using our own solution.

Identifier	Object Type	d_{enc}^{med} (pc)	$d_{enc}^{5\%}$ (pc)	$d_{enc}^{95\%}$ (pc)	v_{enc}^{med} (km s ⁻¹)	$v_{enc}^{5\%}$ (km s ⁻¹)	$v_{enc}^{95\%}$ (km s ⁻¹)	t_{enc} (Myr)	Region/Group
HD 143978	YSO	11.78	8.66	14.75	5.34	4.25	6.34	-18.37	Lupus SFR
2MASS J15480212-4004277	YSO	48.59	24.05	92.47	7.09	6.14	8.69	-23.24	Lupus SFR
2MASS J16081096-3910459	T-Tau star	87.35	77.18	99.87	5.98	5.56	6.96	-34.03	Lupus SFR
RX J1531.3-3329	T-Tau star	91.74	76.20	109.80	5.19	5.02	5.40	-49.99	Lupus SFR/moving group
V1319 Tau	T-Tau star	21.79	18.81	25.18	6.91	6.82	7.06	-28.53	Taurus-Auriga SFR
1RXS J031907.4+393418	T-Tau star	16.45	4.85	43.65	6.11	5.33	6.61	-29.59	Taurus-Auriga SFR(?)
HD 30171	T-Tau star	46.05	15.96	104.13	8.01	6.89	9.39	-43.81	Taurus-Auriga SFR
V1267 Tau	T-Tau star	40.55	22.89	82.41	7.43	6.82	7.83	-49.99	Taurus-Auriga SFR
CFD-53 5235	pre-MS star	77.29	57.99	102.57	4.32	4.09	5.16	-29.41	Sco-Cen SFR
Hn 23	YSO	95.08	83.23	106.12	6.83	6.69	6.99	-45.45	Chamaeleon II SFR
Sz 46N	YSO	79.83	48.90	138.60	7.02	6.49	8.26	-41.89	Chamaeleon II SFR
CM Cha	T-Tau star	85.38	68.48	127.98	7.50	6.95	9.00	-44.20	Chamaeleon II SFR
Hen 3-545	T-Tau star	69.82	53.57	81.21	7.40	7.27	7.59	-46.81	Chamaeleon I SFR
2MASS J11054153-7754441	Emission-line star	69.37	44.58	91.50	8.17	7.89	8.41	-29.75	Chamaeleon I SFR
HD 49855*	rotationally variable star	29.81	22.12	37.38	3.57	3.48	3.65	-36.50	Carina
CD-54 4320	high-pm star	33.46	10.38	77.31	3.98	3.16	4.95	-36.50	Carina
HD 55279*	rotationally variable star	44.62	36.80	55.37	4.23	4.09	4.38	-27.52	Carina
V479 Car*	BY Dra variable	71.66	56.89	89.32	3.43	3.32	3.72	-31.90	Carina
CD-57 1709	rotationally variable star	62.95	49.65	74.38	4.90	4.34	5.63	-32.96	Carina
GJ 1167 A	m dwarf	3.94	2.41	11.16	4.90	2.00	8.06	-2.37	Carina
HD 42270	rotationally variable star	49.75	37.02	65.69	4.69	4.47	4.99	-26.79	Carina
HD 83096*	multiple star	53.64	25.84	90.36	3.57	3.26	4.18	-31.02	Carina
2MASS J09303148-7041479	rotationally variable star	61.85	39.23	85.88	5.20	4.66	5.81	-29.61	Carina-vela
CD-53 2515	rotationally variable star	81.12	24.83	130.13	6.16	4.38	7.73	-34.31	Carina
HD 83096b*	multiple star	44.75	14.19	79.65	4.95	4.46	5.75	-31.86	Carina
CD-54 2644	variable star	59.65	21.37	141.31	3.52	2.37	4.65	-49.14	Carina
CD-49 4008	eclipsing binary star	79.91	63.90	114.89	3.96	2.71	5.12	-38.23	Carina
NOMAD 0269-0122275	eclipsing binary star	66.60	26.68	128.51	5.35	4.96	6.20	-32.89	Carina
NOMAD 0331-0114466	eclipsing binary star	53.03	38.14	69.83	4.82	4.74	4.95	-33.87	Carina
CD-63 408	eclipsing binary star	42.60	40.47	45.43	5.64	5.26	5.86	-27.69	Carina-Vela

Table 6 continued on next page

Table 6 (continued)

Identifier	Object Type	d_{enc}^{med} (pc)	$d_{enc}^{5\%}$ (pc)	$d_{enc}^{95\%}$ (pc)	v_{enc}^{med} (km s ⁻¹)	$v_{enc}^{5\%}$ (km s ⁻¹)	$v_{enc}^{95\%}$ (km s ⁻¹)	t_{enc} (Myr)	Region/Group
HIP 1134*	multiple star	19.77	15.11	24.88	3.92	3.81	4.11	-14.49	Columba
HD 40216*	star	41.58	23.78	53.46	2.50	2.78	1.93	-26.45	Columba
HD 38206*	star	51.73	46.72	61.92	3.36	3.13	3.71	-27.50	Columba
HD 32309*	star	39.89	27.42	61.44	3.60	3.18	4.94	-18.79	Columba
HD 37484*	star	36.44	29.28	48.90	2.72	2.68	2.94	-24.82	Columba
HD 30447*	star	35.48	33.28	39.67	5.09	5.02	5.19	-22.88	Columba
HR 8799(b,c,d,e)*	ellipsoidal variable star & planets	25.55	16.71	51.74	2.81	2.41	4.05	-18.91	Columba
HD 48370	high-pm star	12.92	3.51	21.28	3.46	3.25	3.64	-35.85	Columba
HD 37402	star	11.91	3.46	26.95	4.84	4.30	5.39	-24.46	Columba
HD 32372*	star	46.24	34.25	75.64	4.96	4.43	5.84	-26.56	Columba
kap And A	star	33.09	21.03	44.45	3.34	2.81	3.92	-21.25	Columba
HD 27679	variable star	41.49	31.81	57.46	5.78	5.29	6.22	-23.42	Columba
HD 36329(a,b)	variable binary stars	52.49	49.80	55.04	3.90	3.70	4.07	-26.41	Columba
CD-48 2324	rotationally variable star	71.30	52.14	154.17	3.91	3.33	4.85	-49.99	Columba
RBS 595	rotationally variable star	46.95	39.40	56.70	5.14	4.83	5.45	-25.63	Columba
HD 272836	rotationally variable star	44.67	23.01	84.88	4.59	4.06	5.93	-25.31	Columba
HD 51797	rotationally variable star	66.42	57.30	84.48	2.32	2.14	2.61	-49.99	Columba
HD 39130	star	61.97	33.00	91.33	5.15	4.36	6.16	-29.06	Columba
2MASS J05184616-2756457*	brown dwarf	50.40	36.22	58.38	3.36	1.95	4.02	-24.98	Columba
CD-29 2531	rotationally variable star	63.84	42.44	88.41	5.09	4.45	5.81	-25.02	Columba
TYC 8157-91-1	star	66.54	50.89	85.93	4.48	3.48	5.48	-37.42	Columba
TWA 6	T-Tau star	26.65	20.62	63.84	3.09	2.36	5.11	-20.50	TW Hydra
eps Scl A/B	high-pm star	42.94	14.21	91.39	3.60	1.45	7.53	-12.33	TW Hydra
HR 692	high-pm star	76.53	24.61	176.66	3.45	2.20	7.03	-17.76	TW Hydra
TYC 8083-45-5	rotationally variable star	28.15	16.18	41.75	8.33	7.96	8.63	-32.13	TW Hydra
b Pup	spectroscopic binary	21.35	6.89	163.93	7.35	3.23	15.34	-17.68	no group
KIC 4158372	eruptive variable star	91.66	86.27	95.78	3.61	3.48	3.67	-48.23	no group
KIC 4929016	eruptive variable star	44.62	39.74	48.85	7.03	6.83	7.17	-28.64	no group
HD 189210	eruptive variable star	82.86	80.41	90.57	1.84	1.69	2.51	-49.99	no group
2MASS J04405340+2055471	pre-main sequence star	58.31	41.81	91.40	4.07	3.27	5.73	-20.53	no group
CVSO 229	T-Tau star	84.39	65.27	29.73	16.97	5.39	4.56	-49.99	no group
BD+11 414	T-Tau star	34.61	7.34	89.40	7.73	7.09	9.73	-20.29	no group
2MASS J03581272+0932223	T-Tau star	65.00	36.08	147.59	6.90	3.65	9.15	-49.65	no group
V391 Ori	T-Tau candidate star	50.12	43.24	62.10	3.84	3.77	4.01	-25.52	Orion Nebula Cluster(?)
CD-49 4008	eclipsing binary	70.49	60.24	84.63	3.20	3.12	3.30	-41.89	no group
2MASS J00374306-5846229	brown dwarf	27.99	9.74	54.25	8.36	7.38	9.20	-30.93	no group
2MASS J1411213-211950	low-mass (< 1M _{sol}) star	18.79	5.67	45.69	3.45	1.99	7.11	-11.00	no group
2MASS J03550477-1032415	low-mass (< 1M _{sol}) star	39.68	25.18	52.78	5.09	4.42	5.67	-27.40	no group
HD 24260	white dwarf	59.28	33.59	106.68	7.02	4.46	10.54	-30.00	no group
EGGR 268	white dwarf	3.28	2.27	6.73	24.62	11.93	37.01	-0.65	no group

Table 7. Candidate Systems of Origin for 21/Borisov. Data for these stars was drawn from Gaia DR2 and SIMBAD. These constitute all stars which we find pass within 2 pc at speeds less than 40 km s^{-1} . GJ 4384, EV Lac (Gaia DR2 193426333784036736), and GJ 102 are purported members of the Ursa Major group. Identifiers are as given in Gaia DR2, along with each SIMBAD object type, except for GJ 4384 and GJ 102, for which we take at least part of their astrometry from SIMBAD. Candidates in this table are organized in order of distance.

Identifier	Object Type	d_{ENC}^{med} (pc)	$d_{ENC}^{5\%}$ (pc)	$d_{ENC}^{95\%}$ (pc)	v_{ENC}^{med} (km s^{-1})	$v_{ENC}^{5\%}$ (km s^{-1})	$v_{ENC}^{95\%}$ (km s^{-1})	t_{ENC} (Myr)
G 7-34	flare star	0.21	0.08	0.32	32.61	25.96	38.69	-0.44
GJ 4384	multiple star	0.32	0.11	0.80	19.15	18.74	19.52	-1.46
2MASS J03552337+1133437	brown dwarf	0.44	0.32	0.55	32.06	31.49	32.46	-0.28
5162123155863791744	star	0.64	0.60	0.69	22.50	21.80	23.09	-0.92
411381695718394880	star	0.70	0.65	0.77	29.20	28.75	29.59	-1.36
3338543951096093696	high-pm star	0.72	0.34	1.33	36.75	36.25	37.39	-2.90
2176428914377155200	star	0.81	0.36	1.30	33.28	33.02	33.58	-2.81
207166446152692736	high-pm star	0.85	0.79	0.90	35.15	34.75	35.51	-1.28
193426333784036736	M dwarf/flare star	0.97	0.96	0.97	27.44	27.27	27.61	-0.15
4293318823182081408	BY Dra variable star	1.00	0.99	1.02	35.54	35.27	35.77	-0.14
978301126629450368	star	1.16	0.60	2.15	24.89	24.68	25.13	-5.34
350791183318279552	star	1.26	0.60	2.54	31.64	30.48	32.83	-3.53
217334764042444288	high-pm star	1.44	1.34	1.54	35.61	35.23	36.06	-0.89
5443030196164951168	multiple star	1.54	1.41	1.72	35.18	31.21	39.06	-0.45
2612004014832929536	high-pm star	1.59	0.77	2.53	38.58	38.25	38.93	-3.15
6223838830917236224	high-pm star	1.63	1.47	1.79	13.25	12.99	13.58	-1.95
461259662021372160	star	1.80	1.37	2.37	19.48	16.69	22.16	-6.62
4299703274841464320	high-pm star	1.83	1.38	2.28	20.02	19.42	20.67	-3.15
6501580720836818944	Multiple star	1.92	1.80	2.03	25.09	24.80	25.35	-1.42
GJ 102	M dwarf/flare star	1.98	1.09	5.27	28.26	13.43	44.94	-0.27
6249614407131243648	multiple star	2.00	1.70	2.32	24.45	24.12	24.78	-2.18

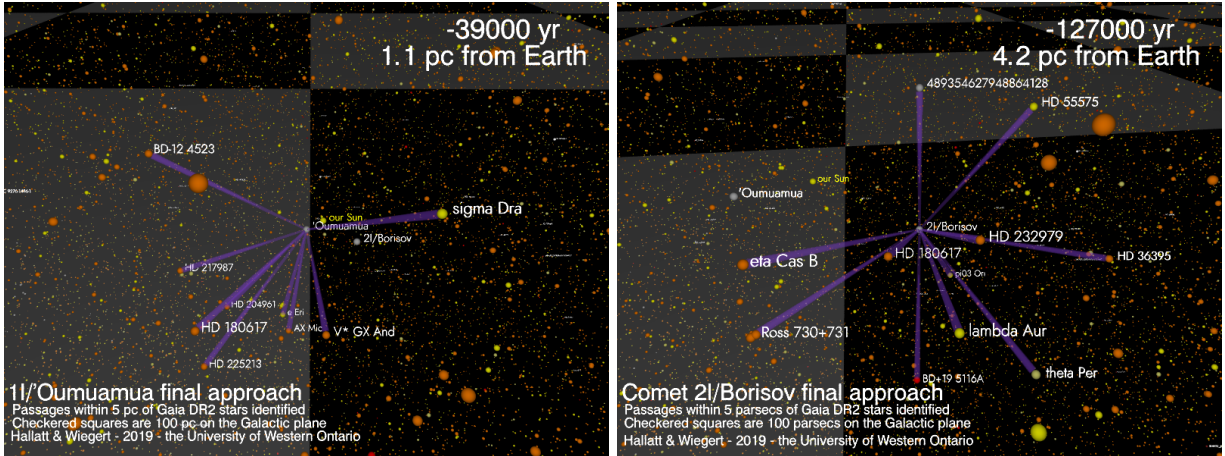


Figure 3. (Animated figure) The final approach of 1I/ʻOumuamua and 2I/Borisov to our Solar System. Passages within 5 pc of members of the Gaia DR2 catalog are identified: note that some local stars (e.g. alpha Centauri) are not in the catalog on not shown. The checkerboard pattern is 100 pc on a side and delineates the Galactic plane. [For review, these are at <http://www.astro.uwo.ca/~wiegert/interstellar/Gaia-Oumuamua-09.mp4> and <http://www.astro.uwo.ca/~wiegert/interstellar/Gaia-Borisov-09.mp4>. Higher resolution versions are also available <http://www.astro.uwo.ca/~wiegert/interstellar/>]

4. CONCLUSIONS

This paper examines the conjecture that ʻOumuamua is much younger than the age of our Galaxy and that it was ejected at low relative velocity with respect to its origin system. The first part of the conjecture is based on the asteroid’s low speed with respect to the LSR (< 12 km/s). Such low velocities are indicative of young $\lesssim 100$ Myr stellar ages from standard age-velocity relations e.g. (Holmberg et al. 2009; Robin et al. 2017). The second part of the conjecture, that ʻOumuamua was ejected at low velocity relative to its parent system, is based on the higher efficiency of most ejection processes at launching material at lower speeds.

Given these assumptions, we first modelled the effects of ‘disk heating’ (gravitational scattering, mostly by giant molecular clouds) on ʻOumuamua’s past trajectory to assess our ability to trace it back to its origin, under these stochastic effects. A backwards integration of ʻOumuamua can only expect to be within 15 pc and 2 km/s of its actual location at -10 Myr, 100 pc and 5 km/s at -50 Myr, and 400 pc and 10 km/s at -100 Myr. This limits our ability to retrace its path, but provides a measure of the size of the envelope of potential origin candidates as we go back in time. If ʻOumuamua was indeed ejected at low speed, that means that the path of its origin system parallels that of ʻOumuamua through the galaxy. Though the origin system’s trajectory is subject to disk heating as well, this system is currently expected to be within 1 kpc of Earth, within the local Orion Arm, and thus accessible in principle to Earth-based telescopes. Thus we can hope to learn more about this unusual asteroid from telescopic study of its parent system, if such system can be identified.

To assess possible local galactic candidate regions, a backwards integration of ʻOumuamua’s trajectory was performed together with systems listed in the Gaia DR2 catalog, SIMBAD, as well as the Catalog of Suspected Nearby Young Stars (Riedel et al. 2018) and members of nearby moving groups compiled in Gagné et al. (2018). Our best candidates are the Carina and Columba moving groups, the Lupus SFR, the T-Tau stars V391 Ori and BD+11 414, and the M dwarf GJ 1167 A. ʻOumuamua passes through at least a considerable subset of the Carina and Columba moving groups at a time comparable to their ages, making it a particularly interesting candidate source regions. The Lupus SFR boasts 4 plausible encounters, 2 of which are with weak-line T-Tau stars, which have been found to be part of an older population of the SFR. This older population may hint to multiple episodes of star formation in the clouds (Makarov 2007) at roughly the time of ʻOumuamua’s encounter, making Lupus another promising candidate.

During the writing of this paper, a second interstellar comet 2I/Borisov was discovered. Though unlikely to be young due to its high velocity with respect to the LSR, we back-integrated it and found three stars in the Ursa Major group (GJ 4384, EV Lac, and GJ 102), one brown dwarf of the AB Dor group (2MASS J03552337+113343), and 8 Gaia DR2 stars (including EV Lac) to have plausible encounters at speeds < 30 kms $^{-1}$ and within 2 pc. The slowest encounter within 2 pc with Gaia stars is with Gaia DR2 223838830917236224, at 13 kms $^{-1}$.

This work has made use of data from the European Space Agency (ESA) mission Gaia (<https://www.cosmos.esa.int/gaia>), processed by the Gaia Data Processing and Analysis Consortium (DPAC, <https://www.cosmos.esa.int/web/gaia/dpac/consortium>). Funding for the DPAC has been provided by national institutions, in particular the institutions participating in the Gaia Multilateral Agreement. This research has made use of the SIMBAD database, operated at CDS, Strasbourg, France. Funding for this work was provided by the Natural Sciences and Engineering Research Council of Canada (Grant no. RGPIN-2018-05659).

REFERENCES

- Alcalá, J., Spezzi, L., N., C., Evans II, N. J., Huard, T. L., K., J. J., B., M., R., S. K., E., C., A., F., D., G., & I., O. (2008). TheSpitzer2d survey of large, nearby, interstellar clouds. x. the chamaeleon II pre-main-sequence population as observed with IRAC and MIPS. *ApJ*, *676*, 427–463. URL: [https://doi.org/10.1086%\\$2F527315](https://doi.org/10.1086%$2F527315). doi:<https://doi.org/10.1086/527315>.
- Bailer-Jones, C. A. L., Farnocchia, D., Meech, K. J., Brassier, R., Micheli, M., Chakrabarti, S., Buie, M. W., & Hainaut, O. R. (2018). Plausible Home Stars of the Interstellar Object ‘Oumuamua Found in Gaia DR2. *AJ*, *156*, 205. doi:<https://doi.org/10.3847/1538-3881/aae3eb>. [arXiv:1809.09009](https://arxiv.org/abs/1809.09009).
- Bertout, C., & Genova, F. (2006). A kinematic study of the Taurus-Auriga T association. *A&A*, *460*, 499–518. doi:<https://doi.org/10.1051/0004-6361:20065842>. [arXiv:astro-ph/0610506](https://arxiv.org/abs/astro-ph/0610506).
- Binney, J., & Tremaine, S. (1987). *Galactic Dynamics*. Princeton: Princeton University Press.
- Bland-Hawthorn, J., & Gerhard, O. (2016). The Galaxy in Context: Structural, Kinematic, and Integrated Properties. *Ann. Rev. Astron. Astrophys.*, *54*, 529–596. doi:<https://doi.org/10.1146/annurev-astro-081915-023441>. [arXiv:1602.07702](https://arxiv.org/abs/1602.07702).
- Bovy, J. (2015). galpy: A python Library for Galactic Dynamics. *Astrophys. J. Suppl.*, *216*, 29. doi:<https://doi.org/10.1088/0067-0049/216/2/29>. [arXiv:1412.3451](https://arxiv.org/abs/1412.3451).
- Brassier, R., & Morbidelli, A. (2013). Oort cloud and Scattered Disc formation during a late dynamical instability in the Solar System. *Icarus*, *225*, 40–49. doi:<https://doi.org/10.1016/j.icarus.2013.03.012>. [arXiv:1303.3098v1](https://arxiv.org/abs/1303.3098v1).
- Broeg, C., Joergens, V., Fernández, M., Husar, D., Hearty, T., Ammler, M., & Neuhäuser, R. (2006). Rotational periods of T Tauri stars in Taurus-Auriga, south of Taurus-Auriga, and in MBM12. *A&A*, *450*, 1135–1148. doi:<https://doi.org/10.1051/0004-6361:20053777>.
- Carpenter, J. M., Bouwman, J., Mamajek, E. E., Meyer, M. R., Hillenbrand, L. A., Backman, D. E., Henning, T., Hines, D. C., Hollenbach, D., Kim, J. S., Moro-Martin, A., Pascucci, I., Silverstone, M. D., Stauffer, J. R., & Wolf, S. (2009). Formation and Evolution of Planetary Systems: Properties of Debris Dust Around Solar-Type Stars. *ApJS*, *181*, 197–226. doi:<https://doi.org/10.1088/0067-0049/181/1/197>. [arXiv:0810.1003](https://arxiv.org/abs/0810.1003).
- Chen, B., Stoughton, C., Smith, J. A., Uomoto, A., Pier, J. R., Yanny, B., Ivezić, Ž., York, D. G., Anderson, J. E., Annis, J., Brinkmann, J., Csabai, I., Fukugita, M., Hindsley, R., Lupton, R., Munn, J. A., & SDSS Collaboration (2001). Stellar Population Studies with the SDSS. I. The Vertical Distribution of Stars in the Milky Way. *ApJ*, *553*, 184–197. doi:<https://doi.org/10.1086/320647>.
- Coşkunoglu, B., Ak, S., Bilir, S., Karaali, S., Yaz, E., Gilmore, G., Seabroke, G. M., Bienaymé, O., Bland-Hawthorn, J., Campbell, R., Freeman, K. C., Gibson, B., Grebel, E. K., Munari, U., Navarro, J. F., Parker, Q. A., Siebert, A., Siviero, A., Steinmetz, M., Watson, F. G., Wyse, R. F. G., & Zwitter, T. (2011). Local stellar kinematics from RAVE data - I. Local standard of rest. *MNRAS*, *412*, 1237–1245. doi:<https://doi.org/10.1111/j.1365-2966.2010.17983.x>. [arXiv:1011.1188](https://arxiv.org/abs/1011.1188).
- Dauphole, B., & Colin, J. (1995). Globular clusters as a new constraint for the potential of our Galaxy. *A&A*, *300*, 117.
- Davies, C. L., Gregory, S. G., & Greaves, J. S. (2014). Accretion discs as regulators of stellar angular momentum evolution in the ONC and Taurus-Auriga. *MNRAS*, *444*, 1157–1176. doi:<https://doi.org/10.1093/mnras/stu1488>. [arXiv:1407.6212](https://arxiv.org/abs/1407.6212).
- Duncan, M., Quinn, T., & Tremaine, S. (1987). The formation and extent of the Solar System comet cloud. *AJ*, *94*, 1330–1338.

- Dybczyński, P. A., & Królikowska, M. (2018). Investigating the dynamical history of the interstellar object 'Oumuamua. *A&A*, *610*, L11.
doi:<https://doi.org/10.1051/0004-6361/201732309>.
arXiv:1711.06618.
- Eubanks, T. M. (2019). High-drag Interstellar Objects and Galactic Dynamical Streams. *ApJL*, *874*, L11.
doi:<https://doi.org/10.3847/2041-8213/ab0f29>.
arXiv:1903.09496.
- Everhart, E. (1985). An efficient integrator that uses Gauss-Radau spacings. In A. Carusi, & G. B. Valsecchi (Eds.), *Dynamics of Comets: Their Origin and Evolution* (pp. 185–202). Dordrecht: Kluwer.
- Feng, F., & Jones, H. R. A. (2018). 'Oumuamua as a Messenger from the Local Association. *ApJL*, *852*, L27.
doi:<https://doi.org/10.3847/2041-8213/aaa404>.
arXiv:1711.08800.
- Fernández, J. A., & Ip, W.-H. (1984). Some dynamical aspects of the accretion of Uranus and Neptune - The exchange of orbital angular momentum with planetesimals. *Icarus*, *58*, 109–120.
- Ferrière, K. M. (2001). The interstellar environment of our galaxy. *Reviews of Modern Physics*, *73*, 1031–1066.
doi:<https://doi.org/10.1103/RevModPhys.73.1031>.
arXiv:astro-ph/0106359.
- Fröhlich, H.-E., Frasca, A., Catanzaro, G., Bonanno, A., Corsaro, E., Molenda-Żakowicz, J., Klutsch, A., & Montes, D. (2012). Magnetic activity and differential rotation in the young Sun-like stars KIC 7985370 and KIC 7765135. *A&A*, *543*, A146.
doi:<https://doi.org/10.1051/0004-6361/201219167>.
arXiv:1205.5721.
- Gagné, J., Mamajek, E. E., Malo, L., Riedel, A., Rodriguez, D., Lafrenière, D., Faherty, J. K., Roy-Loubier, O., Pueyo, L., Robin, A. C., & Doyon, R. (2018). BANYAN. XI. The BANYAN Σ Multivariate Bayesian Algorithm to Identify Members of Young Associations with 150 pc. *ApJ*, *856*, 23.
doi:<https://doi.org/10.3847/1538-4357/aaae09>.
arXiv:1801.09051.
- Gaia Collaboration, Brown, A. G. A., Vallenari, A., Prusti, T., de Bruijne, J. H. J., Babusiaux, C., Bailer-Jones, C. A. L., Biermann, M., Evans, D. W., Eyer, L., Jansen, F., Jordi, C., Klioner, S. A., Lammers, U., Lindegren, L., Luri, X., Mignard, F., Panem, C., Pourbaix, D., Randich, S., Sartoretti, P., Siddiqui, H. I., Soubiran, C., van Leeuwen, F., Walton, N. A., Arenou, F., Bastian, U., Cropper, M., Drimmel, R., Katz, D., Lattanzi, M. G., Bakker, J., Cacciari, C., Castañeda, J., Chaoul, L., Cheek, N., De Angeli, F., Fabricius, C., Guerra, R., Holl, B., Masana, E., Messineo, R., Mowlavi, N., Nienartowicz, K., Panuzzo, P., Portell, J., Riello, M., Seabroke, G. M., Tanga, P., Thévenin, F., Gracia-Abril, G., Comoretto, G., Garcia-Reinaldos, M., Teyssier, D., Altmann, M., Andrae, R., Audard, M., Bellas-Velidis, I., Benson, K., Berthier, J., Blomme, R., Burgess, P., Busso, G., Carry, B., Cellino, A., Clementini, G., Clotet, M., Creevey, O., Davidson, M., De Ridder, J., Delchambre, L., Dell'Oro, A., Ducourant, C., Fernández-Hernández, J., Fouesneau, M., Frémat, Y., Galluccio, L., García-Torres, M., González-Núñez, J., González-Vidal, J. J., Gosset, E., Guy, L. P., Halbwachs, J. L., Hambly, N. C., Harrison, D. L., Hernández, J., Hestroffer, D., Hodgkin, S. T., Hutton, A., Jasiewicz, G., Jean-Antoine-Piccolo, A., Jordan, S., Korn, A. J., Krone-Martins, A., Lanzafame, A. C., Lebzelter, T., Löffler, W., Manteiga, M., Marrese, P. M. et al. (2018). Gaia Data Release 2. Summary of the contents and survey properties. *A&A*, *616*, A1.
doi:<https://doi.org/10.1051/0004-6361/201833051>.
arXiv:1804.09365.

- Gaia Collaboration, Prusti, T., de Bruijne, J. H. J., Brown, A. G. A., Vallenari, A., Babusiaux, C., Bailer-Jones, C. A. L., Bastian, U., Biermann, M., Evans, D. W., Eyer, L., Jansen, F., Jordi, C., Klioner, S. A., Lammers, U., Lindegren, L., Luri, X., Mignard, F., Milligan, D. J., Panem, C., Poinsignon, V., Pourbaix, D., Randich, S., Sarri, G., Sartoretti, P., Siddiqui, H. I., Soubiran, C., Valette, V., van Leeuwen, F., Walton, N. A., Aerts, C., Arenou, F., Cropper, M., Drimmel, R., Høg, E., Katz, D., Lattanzi, M. G., O’Mullane, W., Grebel, E. K., Holland, A. D., Huc, C., Passot, X., Bramante, L., Cacciari, C., Castañeda, J., Chaoul, L., Cheek, N., De Angeli, F., Fabricius, C., Guerra, R., Hernández, J., Jean-Antoine-Piccolo, A., Masana, E., Messineo, R., Mowlavi, N., Nienartowicz, K., Ordóñez-Blanco, D., Panuzzo, P., Portell, J., Richards, P. J., Riello, M., Seabroke, G. M., Tanga, P., Thévenin, F., Torra, J., Els, S. G., Gracia-Abril, G., Comoretto, G., Garcia-Reinaldos, M., Lock, T., Mercier, E., Altmann, M., Andrae, R., Astraatmadja, T. L., Bellas-Velidis, I., Benson, K., Berthier, J., Blomme, R., Busso, G., Carry, B., Cellino, A., Clementini, G., Cowell, S., Creevey, O., Cuypers, J., Davidson, M., De Ridder, J., de Torres, A., Delchambre, L., Dell’Oro, A., Ducourant, C., Frémat, Y., García-Torres, M., Gosset, E., Halbwachs, J. L., Hambly, N. C., Harrison, D. L., Hauser, M., Hestroffer, D. et al. (2016). The Gaia mission. *A&A*, 595, A1. doi:<https://doi.org/10.1051/0004-6361/201629272>. arXiv:1609.04153.
- Gaidos, E. (2018). What and whence II/‘Oumuamua: a contact binary from the debris of a young planetary system? *MNRAS*, 477, 5692–5699. doi:<https://doi.org/10.1093/mnras/sty1072>. arXiv:1712.06721.
- Gaidos, E., Williams, J., & Kraus, A. (2017). Origin of Interstellar Object A/2017 U1 in a Nearby Young Stellar Association? *Research Notes of the American Astronomical Society*, 1, 13. doi:<https://doi.org/10.3847/2515-5172/aa9851>. arXiv:1711.01300.
- Galli, P. A. B., Bertout, C., Teixeira, R., & Ducourant, C. (2013). A kinematic study and membership analysis of the Lupus star-forming region. *A&A*, 558, A77. doi:<https://doi.org/10.1051/0004-6361/201220704>. arXiv:1309.7799.
- Galli, P. A. B., Loinard, L., Ortiz-Léon, G. N., Kounkel, M., Dzib, S. A., Mioduszewski, A. J., Rodríguez, L. F., Hartmann, L., Teixeira, R., Torres, R. M., Rivera, J. L., Boden, A. F., Evans, N. J., II, Briceño, C., Tobin, J. J., & Heyer, M. (2018). The Gould’s Belt Distances Survey (GOBELINS). IV. Distance, Depth, and Kinematics of the Taurus Star-forming Region. *ApJ*, 859, 33. doi:<https://doi.org/10.3847/1538-4357/aabf91>. arXiv:1805.09357.
- Gammie, C. F., Ostriker, J. P., & Jog, C. J. (1991). The Velocity Dispersion of Giant Molecular Clouds. II. Mathematical and Numerical Refinements. *ApJ*, 378, 565. doi:<https://doi.org/10.1086/170458>.
- Gillessen, S., Eisenhauer, F., Trippe, S., Alexander, T., Genzel, R., Martins, F., & Ott, T. (2009). Monitoring Stellar Orbits Around the Massive Black Hole in the Galactic Center. *ApJ*, 692, 1075–1109. doi:<https://doi.org/10.1088/0004-637X/692/2/1075>. arXiv:0810.4674.
- Guo, J., Zhao, J., Tziamtzis, A., Liu, J., Li, L., Zhang, Y., Hou, Y., & Wang, Y. (2015). White dwarfs identified in LAMOST DR 2. *MNRAS*, 454, 2787–2797. doi:<https://doi.org/10.1093/mnras/stv2104>.
- Guzik, P., Drahus, M., Rusek, K., Waniak, W., Cannizzaro, G., & Pastor-Marazuela, I. (2019). Initial characterization of interstellar comet 2I/Borisov. *Nature Astronomy*, . doi:<https://doi.org/10.1038/s41550-019-0931-8>.
- Hambálek, Ā., VaĀko, M., Paunzen, E., & Smalley, B. (2019). T Tauri stars in the SuperWASP and NSVS surveys. *MNRAS*, 483, 1642–1654. doi:<https://doi.org/10.1093/mnras/sty3151>. arXiv:1811.08655.
- Holberg, J. B., Oswalt, T. D., & Sion, E. M. (2002). A Determination of the Local Density of White Dwarf Stars. *ApJ*, 571, 512–518. doi:<https://doi.org/10.1086/339842>. arXiv:astro-ph/0102120.
- Holmberg, J., Nordström, B., & Andersen, J. (2009). The Geneva-Copenhagen survey of the solar neighbourhood. III. Improved distances, ages, and kinematics. *A&A*, 501, 941–947. doi:<https://doi.org/10.1051/0004-6361/200811191>. arXiv:0811.3982.
- Hughes, J., Hartigan, P., Krautter, J., & Kelemen, J. (1994). The stellar population of the Lupus clouds. *AJ*, 108, 1071–1090. doi:<https://doi.org/10.1086/117135>.

- Jackson, A., Tamayo, D., Hammond, N., Ali-Dib, M., & Rein, H. (2018). Ejection of rocky and icy material from binary star systems: implications for the origin and composition of 1I/'Oumuamua. *MNRAS*, *478*, L49–L53. doi:<https://doi.org/10.1093/mnras/sly033>. arXiv:1712.04435v2.
- Jog, C. J., & Ostriker, J. P. (1988). The Velocity Dispersion of the Giant Molecular Clouds: A Viscous Origin. *ApJ*, *328*, 404. doi:<https://doi.org/10.1086/166302>.
- Kenyon, S. J., Dobrzycka, D., & Hartmann, L. (1994). A new optical extinction law and distance estimate for the Taurus-Auriga molecular cloud. *AJ*, *108*, 1872–1880. doi:<https://doi.org/10.1086/117200>.
- Kraus, A. L., Herczeg, G. J., Rizzuto, A. C., Mann, A. W., Slesnick, C. L., Carpenter, J. M., Hillenbrand, L. A., & Mamajek, E. E. (2017). The Greater Taurus-Auriga Ecosystem. I. There is a Distributed Older Population. *ApJ*, *838*, 150. doi:<https://doi.org/10.3847/1538-4357/aa62a0>. arXiv:1702.04341.
- Li, J. Z., & Hu, J. Y. (1998). Newly discovered candidate weak-line T Tauri stars in the surrounding area of the Taurus-Auriga region. *Astron. Astrophys. Suppl.*, *132*, 173–179. doi:<https://doi.org/10.1051/aas:1998288>.
- Lombardi, M., Lada, C. J., & Alves, J. (2008). Hipparcos distance estimates of the Ophiuchus and the Lupus cloud complexes. *A&A*, *480*, 785–792. doi:<https://doi.org/10.1051/0004-6361/20079110>. arXiv:0801.3346.
- Luhman, K. (2018). The Stellar Membership of the Taurus Star-forming Region. *AJ*, *156*, 271.
- Makarov, V. (2007). The Lupus Association of Pre-Main-Sequence Stars: Clues to Star Formation Scattered in Space and Time. *ApJ*, *658*, 480–486. doi:<https://doi.org/10.1086/511261>.
- Mamajek, E. (2017). Kinematics of the Interstellar Vagabond 1I/'Oumuamua (A/2017 U1). *Research Notes of the American Astronomical Society*, *1*, 21. doi:<https://doi.org/10.3847/2515-5172/aa9bdc>. arXiv:1710.11364.
- Meech, K. J., Weryk, R., Micheli, M., Kleyna, J. T., Hainaut, O. R., Jedicke, R., Wainscoat, R. J., Chambers, K. C., Keane, J. V., Petric, A., Denneau, L., Magnier, E., Berger, T., Huber, M. E., Flewelling, H., Waters, C., Schunova-Lilly, E., & Chastel, S. (2017). A brief visit from a red and extremely elongated interstellar asteroid. *Nature*, *552*, 378–381. doi:<https://doi.org/10.1038/nature25020>.
- Menten, K. M., Reid, M. J., Forbrich, J., & Brunthaler, A. (2007). The distance to the Orion Nebula. *A&A*, *474*, 515–520. doi:<https://doi.org/10.1051/0004-6361:20078247>. arXiv:0709.0485.
- Micheli, M., Farnocchia, D., Meech, K. J., Buie, M. W., Hainaut, O. R., Prialnik, D., Schörghofer, N., Weaver, H. A., Chodas, P. W., Kleyna, J. T., Weryk, R., Wainscoat, R. J., Ebeling, H., Keane, J. V., Chambers, K. C., Koschny, D., & Petropoulos, A. E. (2018). Non-gravitational acceleration in the trajectory of 1I/2017 U1 ('Oumuamua). *Nature*, *559*, 223–226. doi:<https://doi.org/10.1038/s41586-018-0254-4>.
- Mihalas, D., & Binney, J. (1981). *Galactic Astronomy*. New York: W. H. Freeman and Co.
- Miyamoto, M., & Nagai, R. (1975). Three-dimensional models for the distribution of mass in galaxies. *Publ. Astr. Soc. Japan*, *27*, 533–543.
- Moro-Martín, A., Turner, E., & Loeb, A. (2009). Will the Large Synoptic Survey Telescope detect extra-solar planetesimals entering the solar system? *AJ*, *704*, 733–742. doi:<https://doi.org/10.1088/0004-637x/704/1/733>. arXiv:0908.3948v2.
- Mulders, G. D., Pascucci, I., Manara, C. F., Testi, L., Herczeg, G. J., Henning, T., Mohanty, S., & Lodato, G. (2017). Constraints from Dust Mass and Mass Accretion Rate Measurements on Angular Momentum Transport in Protoplanetary Disks. *ApJ*, *847*, 31. doi:<https://doi.org/10.3847/1538-4357/aa8906>. arXiv:1708.09464.
- Murray, N., Weingartner, J. C., & Capobianco, C. (2004). On the Flux of Extrasolar Dust in Earth's Atmosphere. *ApJ*, *600*, 804–827. doi:<https://doi.org/10.1086/380117>. arXiv:arXiv:astro-ph/0309805.
- Nguyen, D. C., Brandeker, A., van Kerkwijk, M. H., & Jayawardhana, R. (2012). Close Companions to Young Stars. I. A Large Spectroscopic Survey in Chamaeleon I and Taurus-Auriga. *ApJ*, *745*, 119. doi:<https://doi.org/10.1088/0004-637X/745/2/119>. arXiv:1112.0002.
- Oswalt, J. B. H. T. D., Sion, E. M., & McCook, G. P. (2016). The 25 Parsec Local White Dwarf Population. *arXiv e-prints*, . arXiv:1606.01236.
- Palla, F., & Stahler, S. W. (2002). Star Formation in Space and Time: Taurus-Auriga. *ApJ*, *581*, 1194–1203. doi:<https://doi.org/10.1086/344293>. arXiv:astro-ph/0208554.

- Pecaut, M. J., Mamajek, E. E., & Bubar, E. J. (2012). A Revised Age for Upper Scorpius and the Star Formation History among the F-type Members of the Scorpius-Centaurus OB Association. *ApJ*, *746*, 154. doi:<https://doi.org/10.1088/0004-637X/746/2/154>. arXiv:1112.1695.
- Portail, M., Wegg, C., Gerhard, O., & Martínez-Valpuesta, I. (2015). Made-to-measure models of the Galactic box/peanut bulge: stellar and total mass in the bulge region. *MNRAS*, *448*, 713–731. doi:<https://doi.org/10.1093/mnras/stv058>. arXiv:1502.00633.
- Portegies Zwart, S., Torres, S., Pelupessy, I., Bédorf, J., & Cai, M. X. (2018). The origin of interstellar asteroidal objects like 1I/2017 U1 ‘Oumuamua. *MNRAS*, *479*, L17–L22. doi:<https://doi.org/10.1093/mnrasl/sly088>. arXiv:1711.03558.
- Preibisch, T., & Mamajek, E. (2008). The Nearest OB Association: Scorpius-Centaurus (Sco OB2). In B. Reipurth (Ed.), *Handbook of Star Forming Regions, Volume II* (p. 235).
- Rafikov, R. (2018). 1I/2017 ‘Oumuamua-like Interstellar Asteroids as Possible Messengers from Dead Stars. *AJ*, *861*, 35. doi:<https://doi.org/10.3847/1538-4357/aac5ef>. arXiv:1801.02658v3.
- Reid, M. J., & Brunthaler, A. (2004). The Proper Motion of Sagittarius A*. II. The Mass of Sagittarius A*. *ApJ*, *616*, 872–884. doi:<https://doi.org/10.1086/424960>. arXiv:astro-ph/0408107.
- Reipurth, B. (2008). *Handbook of Star Forming Regions, Volume II: The Southern Sky*.
- Riedel, A. R., Blunt, S. C., Lambrides, E. L., Rice, E. L., Cruz, K. L., & Faherty, J. K. (2017). LACEwING: A New Moving Group Analysis Code. *AJ*, *153*, 95. doi:<https://doi.org/10.3847/1538-3881/153/3/95>. arXiv:1702.02219.
- Riedel, A. R., Blunt, S. C., Lambrides, E. L., Rice, E. L., Cruz, K. L., & Faherty, J. K. (2018). VizieR Online Data Catalog: Catalog of Suspected Nearby Young Stars (Riedel+, 2017). *VizieR Online Data Catalog*, *515*.
- Robin, A. C., Bienaymé, O., Fernández-Trincado, J. G., & Reylé, C. (2017). Kinematics of the local disk from the RAVE survey and the Gaia first data release. *A&A*, *605*, A1. doi:<https://doi.org/10.1051/0004-6361/201630217>. arXiv:1704.06274.
- Schönrich, R., Binney, J., & Dehnen, W. (2010). Local kinematics and the local standard of rest. *MNRAS*, *403*, 1829–1833. doi:<https://doi.org/10.1111/j.1365-2966.2010.16253.x>. arXiv:0912.3693v1.
- Song, I., Zuckerman, B., & Bessell, M. S. (2012). New Members of the Scorpius-Centaurus Complex and Ages of Its Sub-regions. *AJ*, *144*, 8. doi:<https://doi.org/10.1088/0004-6256/144/1/8>. arXiv:1204.5715.
- Spezzi, L., M., A. J., E., C., A., F., D., G., I., O., N., C., J., E. N., L., H. T., K., J. J., B., M., & R., S. K. (2008). The young population of the chamaeleon II dark cloud. *ApJ*, *680*, 1295–1318. URL: <https://doi.org/10.1086%2F587931>. doi:<https://doi.org/10.1086/587931>.
- Szegedi-Elek, E., Kun, M., Reipurth, B., Pál, A., Balázs, L. G., & Willman, M. (2013). A New H α Emission-line Survey in the Orion Nebula Cluster. *Astrophys. J. Suppl.*, *208*, 28. doi:<https://doi.org/10.1088/0067-0049/208/2/28>. arXiv:1308.1812.
- Torres, R. M., Loinard, L., Mioduszewski, A. J., Boden, A. F., Franco-Hernández, R., Vlemmings, W. H. T., & Rodríguez, L. F. (2012). VLBA Determination of the Distance to nearby Star-forming Regions. V. Dynamical Mass, Distance, and Radio Structure of V773 Tau A. *ApJ*, *747*, 18. doi:<https://doi.org/10.1088/0004-637X/747/1/18>. arXiv:1112.0114.
- Torres, R. M., Loinard, L., Mioduszewski, A. J., & Rodríguez, L. F. (2007). VLBA Determination of the Distance to Nearby Star-forming Regions. II. Hubble 4 and HDE 283572 in Taurus. *ApJ*, *671*, 1813–1819. doi:<https://doi.org/10.1086/522924>. arXiv:0708.4403.
- Voirin, J., Manara, C. F., & Prusti, T. (2018). A revised estimate of the distance to the clouds in the Chamaeleon complex using the Tycho-Gaia Astrometric Solution. *A&A*, *610*, A64. doi:<https://doi.org/10.1051/0004-6361/201731153>. arXiv:1710.04528.
- Wenger, M., Ochsenbein, F., Egret, D., Dubois, P., Bonnarel, F., Borde, S., Genova, F., Jasniewicz, G., Laloë, S., Lesteven, S., & Monier, R. (2000). The SIMBAD astronomical database. The CDS reference database for astronomical objects. *A&AS*, *143*, 9–22. doi:<https://doi.org/10.1051/aas:2000332>. arXiv:astro-ph/0002110.
- Wielen, R. (1977). The Diffusion of Stellar Orbits Derived from the Observed Age-Dependence of the Velocity Dispersion. *A&A*, *60*, 263–275.

- Wright, N. J., & Mamajek, E. E. (2018). The kinematics of the Scorpius-Centaurus OB association from Gaia DR1. *Monthly Notices of the Royal Astronomical Society*, *476*, 381–398. URL: <https://doi.org/10.1093/mnras/sty207>. doi:<https://doi.org/10.1093/mnras/sty207>. arXiv:1801.08540.
- Zhang, Q. (2018). Prospects for Backtracing 1I/'Oumuamua and Future Interstellar Objects. *Astrophys. J. Lett.*, *852*, L13. doi:<https://doi.org/10.3847/2041-8213/aaa2f7>. arXiv:1712.08059.
- Zuluaga, J. I., Sánchez-Hernández, O., Sucerquia, M., & Ferrín, I. (2018). A General Method for Assessing the Origin of Interstellar Small Bodies: The Case of 1I/2017 U1 ('Oumuamua). *AJ*, *155*, 236. doi:<https://doi.org/10.3847/1538-3881/aabd7c>. arXiv:1711.09397.